ITUPublications

International Telecommunication Union
Radiocommunication Sector

Report ITU-R P.2402-1

(06/2026)

P Series: Radio-wave propagation

A method to predict the statistics of clutter loss for Earth-space and aeronautical paths

Foreword

The role of the Radiocommunication Sector is to ensure the rational, equitable, efficient and economical use of the radio-frequency spectrum by all radiocommunication services, including satellite services, and carry out studies without limit of frequency range on the basis of which Recommendations are adopted.

The regulatory and policy functions of the Radiocommunication Sector are performed by World and Regional Radiocommunication Conferences and Radiocommunication Assemblies supported by Study Groups.

Policy on Intellectual Property Right (IPR)

ITU-R policy on IPR is described in the Common Patent Policy for ITU-T/ITU-R/ISO/IEC referenced in Resolution ITU-R 1. Forms to be used for the submission of patent statements and licensing declarations by patent holders are available from https://www.itu.int/ITU-R/go/patents/en where the Guidelines for Implementation of the Common Patent Policy for ITU-T/ITU-R/ISO/IEC and the ITU-R patent information database can also be found.

Series of ITU-R Reports

(Also available online at https://www.itu.int/publ/R-REP/en)

Series	Title
BO	Satellite delivery
BR	Recording for production, archival and play-out; film for television
BS	Broadcasting service (sound)
BT	Broadcasting service (television)
F	Fixed service
M	Mobile, radiodetermination, amateur and related satellite services
P	**Radio-wave propagation**
RA	Radio astronomy
RS	Remote sensing systems
S	Fixed-satellite service
SA	Space applications and meteorology
SF	Frequency sharing and coordination between fixed-satellite and fixed service systems
SM	Spectrum management
TF	Time signals and frequency standards emissions

Note*: This ITU-R Report was approved in English by the Study Group under the procedure detailed in Resolution ITU-R 1.*

Electronic Publication
Geneva, 2026

REPORT ITU-R P.2402-1

A method to predict the statistics of clutter loss for Earth-space and aeronautical paths

(2017-2026)

Scope

This Report describes stochastic methods for clutter losses and provides statistical distributions of clutter loss for reference environments. It also provides the background material for Recommendation ITU-R P.2108, § 3.3 and a reference for future studies.

It is organized in two chapters. Chapter 1 introduces the description of the physical process of the clutter loss, its stochastic aspects and defines the framework for its statistical modelling. Chapter 2 provides a stochastic model that can be used to generate distributions of clutter loss using as input a statistical description of the clutter environment.

TABLE OF CONTENTS

Page

CHAPTER 1

General description of the clutter loss along Earth-space paths

1 Introduction and assumptions

The focus in this chapter is the use of the clutter model for analyses of interference between a transmitter on ground (the interfering station) and a receiver in space (the interfered station) (see Fig. 1). This type of analysis shall provide results applicable to the most general range of cases and therefore a stochastic approach is considered as more appropriate than a deterministic characterisation of a certain environment using other methods (e.g. ray-tracing or experimental characterisation). However, these alternative methods are considered essential for the validation and verification of the assumptions of the stochastic models.

The main effect of a clutter environment is, on one hand, to reduce the energy of the signal transmitted directly towards the station in space and, on the other hand, to create additional propagation paths between the stations on Earth and in space (see Fig. 1). In this configuration, the distance between a transmitter on the ground and receiver is very large and the clutter is in the environment around the transmitter on the ground. Therefore, all the components of the electromagnetic (EM) field generated by the clutter arrive at the receiver in space with the same direction of the direct path from the transmitter to the receiver.

For the scope of interference analyses, it can be assumed that the phases of the waves arriving at the station in space are randomly distributed, so the total power is the sum of the power of each wave.

The discussion in this chapter starts in a general way, then methods to use clutter loss parameters with specific antenna patterns are introduced.

FIGURE 1

Ground station surrounded by clutter interfering on a station in space

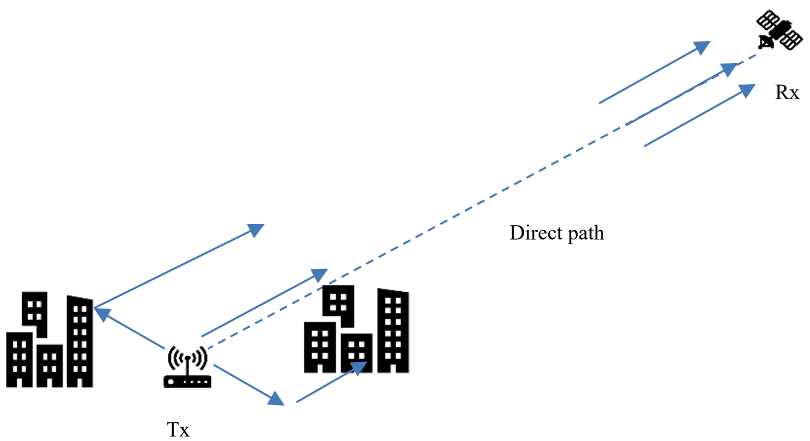

The specific local clutter environment can be described statistically using the set[1] of its all-possible configurations, ENV_{cl}. Section 2 provides information on the procedure for its statistical characterisation using survey points.

In the following the plane electromagnetic wave generated by clutter effects will be described using ray notation.

---

[1] In this chapter, a set A is represented as {A} and it contains elements, *e*.

The ray along the direct path between transmitter and receiver is chosen as the reference direction for clutter loss and therefore it is identified by the index $i = 1$. The direct path is described by (θ_1, ϕ_1), where $\theta_1 \equiv \theta$ is the elevation angle with respect to local horizontal plane, and $\phi_1 \equiv \phi$ is the azimuth angle with respect to the North direction.

The clutter along the path affects each ray with three different propagation effects:

– Edge diffraction by clutter.

– Reflection from a surface near the transmitter and possible subsequent diffractions, reflections and diffuse scattering by clutter along the path, resulting in propagation along a direction parallel to the direct path, see Fig. 2.

FIGURE 2

Example of reflections of the signal transmitted by a station on the Earth towards a space station

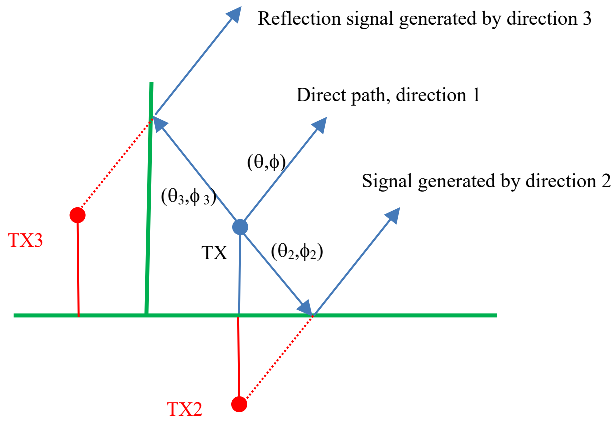

Note to Fig. 2: Red indicates specular images of the transmitter generated by reflections.

– Diffuse scattering[2] from a rough surface near the transmitter and in case subsequent diffractions, reflections and diffuse scattering by clutter along the path, resulting in propagation along a direction parallel to the direct path. See Fig. 3.

FIGURE 3

Example of diffuse scattering of the signal transmitted by a station on the Earth towards a space station

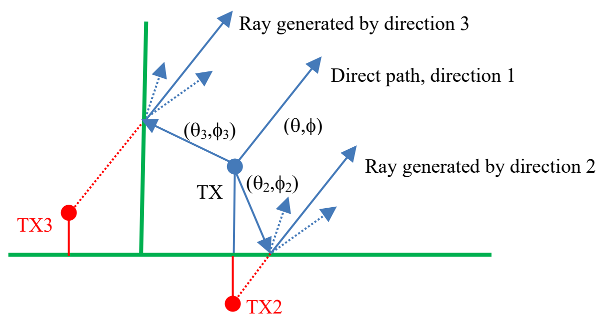

[2] In the following diffuse scattering is assumed to be significantly lower than the other terms (diffraction and reflection) and it is not included in the analysis. However, the notation for scattering is like the one for reflection, so in case the following methods can be extended to also include this effect.

Note to Fig. 3: Red indicates specular images of the transmitter on ground generated by scattering of signal transmitted along a direction different from the direct path.

Each ray leaving the ground transmitter can generate one or more rays arriving at the receiver in space. There are N_L rays leaving the receiver and generating one or more rays ($n_i \geq 1, i = 1, 2 \cdots N_L$) arriving at the receiver. The total number of rays arriving at the receiver is N_R.

$$N_R = \sum_1^{N_L} n_i \tag{1}$$

The geometrical configuration of the transmitter, the clutter environment and the receiver identify the N_L rays leaving the transmitter and contributing to the transmission signal towards the station in space along direction (θ, ϕ). They are the elements of the set RAY_L:

$$RAY_L = \{ray_1, ray_2 \cdots ray_{N_L}\} \tag{2}$$

where:

ray_i : ray leaving the transmitter along direction (θ_i, ϕ_i)

ray_1 : along the direct path (ray_D).

RAY_L can be described in general as the result of the application of a functional $\mathcal{F}_l$, on the direct path direction (θ_1, ϕ_1), the specific clutter environment e_{cl} and the position of the ground transmitter within the clutter, loc_{gt} (e.g. transmitter distance and height). In the following, the equivalence $(\theta, \phi) \equiv (\theta_1, \phi_1)$ is used:

$$RAY_L = \mathcal{F}_l\left((\theta, \phi), e_{cl}, loc_{gt}\right) \tag{3}$$

Because of propagation effects described above, each ray of RAY_L generates one or more rays arriving at the receiver, that constitute the set RAY_R. This set contains ray_1 and eventually other rays.

$$RAY_R = \{ray_{R1}, ray_{R2} \cdots ray_{RN_R}\} \tag{4}$$

where $ray_{R1} = ray_1 = ray_D$ represents the ray propagating along the direct path and N_R is the total number of rays arriving at the receiver (see equation (1)). The other rays include also the case of rays generated by reflections of ray_1.[3]

The mapping between the rays leaving the transmitter and the rays propagating to the receiver at frequency f can be described in general using a functional operator $\mathcal{F}_r$:

$$RAY_R = \mathcal{F}_r(RAY_L, f) \tag{5}$$

For example, if only the direct ray, ray_1, and its reflection ray_{refl} are considered, then $RAY_L = \{ray_1\}$ and $RAY_r = \{ray_1, ray_{refl}\}$. This definition could be extended to include also all the rays leaving the receiver which do not propagate to the receiver by mapping these set to an empty set.

The clutter propagation effects determine a variation of power of the EM wave arriving at the space station, P_{rcl}, with respect to the power received in absence of clutter, P_{rncl}.

$$P_{rcl} = P_{rncl}/l_{cl}(\theta, \phi, f) \qquad \text{W} \tag{6}$$

[3] The case of a ray not arriving at the receiver is treated as a mathematical limit of attenuation tending to infinite.

$l_{cl}(\theta, \phi, f)$, is the clutter loss[4] in natural units with $L_{cl}(\theta, \phi, f) = 10\log_{10}\left(l_{cl}(\theta, \phi, f)\right)$ dB.

Clutter loss l_{cl} can be described in general as the result of the application of a functional $\mathcal{F}_{cl}$ on the set of rays arriving at the receiver $\{RAY_r\}$ along the direct path and the frequency of the link:

$$l_{cl}\big((\theta, \phi), f\big) = \mathcal{F}_{cl}(\,RAY_R) \tag{7}$$

By using equations (5) and (3), this functional can be written as:

$$l_{cl}(\theta, \phi, f) = \mathcal{F}_{cl}(\,e^*{}_{cl}) \tag{8}$$

where $e^*{}_{cl}$=$\mathcal{F}_r\left(\mathcal{F}_l\left((\theta, \phi), e_{cl}, loc_{gt}\right), f\right)$ is an equivalent electromagnetic clutter environment incorporating the dependency of clutter loss on the direct path direction (θ, ϕ), specific clutter environment, e_{cl}, transmitter position loc_{gt} and frequency f. Therefore, the definition of the set or rays leaving the transmitter and contributing to the signal arriving at the receiver, RAY_L , is the basis for the assessment of the clutter loss.

2 Calculation of the power towards the station in space due to clutter

This section reviews the definitions for calculating the total power of all the rays generated by clutter on ground and arriving at the space station, assuming at first isotropic antennas on both transmitter and receiver (as in Recommendation ITU-R P.341) and then extending it to the case of any other (i.e. non-isotropic) transmitter antenna. Because of the distance only rays along the direction of the direct path are received by a station in space.

In the absence of clutter, the station in space receives only the ray transmitted along the direct path, and the received power is:

$$P_r(\theta, \phi) = P_t - L_{bf} \qquad \text{dBW} \tag{9}$$

where: P_t is the power at the TX antenna input terminal in dBW and $L_{bf} = 20\log_{10}\left(4\pi\frac{d}{\lambda}\right)$ is the free space loss dB, d is the distance between transmitter and receiver m along the direct path and λ is the wavelength m.

As discussed in the previous section, the presence of clutter around the station on the Earth can generate: 1) a reduction of the power of the ray along the direct path due to diffraction, $ray_{R1} = ray_1$ and 2) an increase of the power due to the arrival at the space station of the other rays in RAY_R (see rays with index larger than 1 in equation (4)) generated by reflections.

In the following the total received power is calculated as the power sum of each component assuming that the phases of all the rays arriving at the receiver are randomly distributed with a uniform probability density function.

These two cases are discussed separately.

---

[4] According to this definition of loss, values $l_{cl} > 1$ and $l_{cl} < 1$ represent reduction or increase of, respectively. Clutter loss can be lower or larger than 1 depending on the combination of the different rays along all the possible propagation paths (e.g. reduction in the case of clutter diffraction only along the direct path or increase in the case of direct path and clutter lossless reflection from the ground).

2.1 Isotropic antenna case

2.1.1 Reduction of power due to clutter along the direct path (isotropic antenna)

In this case, the power received by the station in space with an isotropic antenna is:

$$p_{r1}(\theta,\phi) = p_t \cdot \frac{1}{l_d(\theta,\phi)} \cdot \left(\frac{\lambda}{4\pi d}\right)^2 \qquad \text{W} \qquad (10)$$

where ray_d is transmitted along the direct path and $l_d(\theta,\phi) \geq 1$ is the loss due to clutter diffraction along the direct path[5].

Equation (10) can be expressed in dB:

$$P_{r1}(\theta,\phi) = P_t - L_d(\theta,\phi) - L_{bf} \qquad \text{dBW} \qquad (11)$$

where $L_{bf} = 20\log_{10}\left(\frac{4\pi d}{\lambda}\right)$ is the free space loss dB, $L_{d1}(\theta,\phi) = 10\log_{10}\big(l_d(\theta,\phi)\big)$ and $L_{d1} \geq 0$ dB.

2.1.2 Additional power due to other rays arriving at the receiver (isotropic antenna)

The set of rays arriving at the receiver, RAY_R, can include a number of rays, ray_{Ri} (see equation (4)) other than the direct ray and originated by a specific ray leaving the transmitter, ray_i.

This creates a subset RAY_{Ri} containing all the received rays that were originated by transmitted ray ray_i.

$$RAY_{Ri} = \left\{ray_{R1i}, ray_{R2i} \cdots ray_{Rn_i i}\right\} \qquad (12)$$

where $i = 1 .. N_L$ and Rn_i is the number of received rays generated by the transmitted ray ray_i via reflections and diffraction. For example, the direct ray $ray_d \equiv ray_1$ can generate via reflections an additional ray, $ray_{R11} \equiv ray_{Rd}$.

The power of ray_{Rji} at the input of the antenna of the station in space, transmitted from ground with an isotropic antenna is:

$$p_{Rji}(\theta,\phi) = \frac{p_t}{4\pi} \cdot \frac{1}{l_{Rji}} \cdot \frac{1}{d_{ji}^2} \cdot \frac{\lambda^2}{4\pi} \qquad \text{W} \qquad (13)$$

where $l_{Rji} \geq 1$ is the loss[5] of ray ray_{Rji} and d_{ji} is the distance travelled by ray ray_{rji} to arrive at the station in space. If the distance between transmitter and receiver is much larger than the distance between transmitter and clutter on the Earth, the overall free space loss of ray_{rji} can be approximated by the free space loss of the direct path and:

$$p_{Rji}(\theta,\phi) \approx p_t \cdot \frac{1}{l_{Rji}} \cdot \left(\frac{\lambda}{4\pi d}\right)^2 \qquad \text{W} \qquad (14)$$

The total power at the receiver due to all rays generated by ray_i along the direct path, $p_{Ri}(\theta,\phi)$, can be calculated assuming power combination[6].

---

[5] $l_d(\theta,\phi)$ can be lower than 1 due to oscillations of diffraction losses around 1 when the ray is in the region between Fresnel line of sight and optical line of sight. This case is not considered for the sake of simplicity.

[6] This assumes that the phases of all rays arriving at the receiver have a random distribution with a uniform probability density function.

$$p_{Ri}(\theta,\phi)=\sum_{j=1}^{n_i} p_t\cdot\frac{1}{l_{Rji}}\cdot\left(\frac{\lambda}{4\pi d}\right)^2=p_t\cdot\frac{1}{l_{Ri}}\cdot\left(\frac{\lambda}{4\pi d}\right)^2 \qquad \text{W} \qquad (15)$$

where $l_{Ri}(\theta,\phi)=1/\sum_{j=1}^{n_i}\frac{1}{l_{Rji}}$ is the overall loss along direction (θ,ϕ) of all n_i rays generated by the ray_i leaving the transmitter.

For example, $l_{R1}(\theta,\phi)$ identifies the clutter loss of the rays generated from reflections of direct ray ray_D. In the following $l_{Rd}\equiv l_{R1}$.

This equation can be expressed in dBW.

$$P_{Ri}(\theta,\phi)=P_T-L_{Ri}(\theta,\phi)-L_{bf} \qquad \text{dBW} \qquad (16)$$

where $L_{Ri}(\theta,\phi)=10\log_{10}\left(l_{Ri}(\theta,\phi)\right)\geq 0$ dB (see footnote 5).

2.1.3 Combination of direct ray and other rays (isotropic antenna)

The total power of rays at the receiver due to all rays transmitted from the ground can be calculated assuming power combination (see footnote 5) of the contributions from the direct ray, ray_1 (see equation (10)), and from the rays generated all other rays, transmitted along different directions, ray_i (see equation (15)).

$$p_R(\theta,\phi)=p_t\cdot\frac{1}{l_d(\theta,\phi)}\cdot\left(\frac{\lambda}{4\pi d}\right)^2+\frac{1}{l_{Rd}(\theta,\phi)}\cdot\left(\frac{\lambda}{4\pi d}\right)^2+\sum_{i=2}^{N_L} p_t\cdot\frac{1}{l_{Ri}(\theta,\phi)}\cdot\left(\frac{\lambda}{4\pi d}\right)^2$$
$$=p_t\cdot\frac{1}{l_{cl}}\cdot\left(\frac{\lambda}{4\pi d}\right)^2 \qquad \text{W} \qquad (17)$$

where l_{Ri} is defined in equation (15) and l_d in equation (10) and $l_{R1}\equiv l_{Rd}$ is the ray generated by ray_d after a reflection.

The total clutter loss along the direction (θ,ϕ), with respect to the case of power received along the direct path in absence of clutter and ground reflections, is:

$$\frac{p_t}{p_R(\theta,\phi)}\left(\frac{\lambda}{4\pi d}\right)^2\equiv l_{cl}(\theta,\phi)=1/\left(\frac{1}{l_{cld}}+\sum_{i=2}^{N_L}\frac{1}{l_{Ri}}\right) \qquad (18)$$

with $l_{cl}\geq 1/(1+N_L)$ and $l_{cld}=1/\left(\frac{1}{l_d}+\frac{1}{l_{Rd}}\right)$ is the total clutter loss of the direct ray.

The equality applies to the ideal case of unobstructed direct path and N_L rays reflected without losses. Values of $l_{cl}<1$ indicate an increase of power received in space with respect to the case of absence of clutter.

This equation can be expressed in dBW.

$$P_r(\theta,\phi)=P_t-L_{cl}(\theta,\phi)-L_{bf} \qquad \text{dBW} \qquad (19)$$

where $L_{cl}(\theta,\phi)=10\log_{10}\left(l_{cl}(\theta,\phi)\right)$ dB is the clutter loss relative to free space.

with $L_{cl}\geq -10\log_{10}(1+N_L)$.

In agreement to Recommendation ITU-R P.341, the basic transmission loss is:

$$L_b(\theta,\phi)=L_{cl}(\theta,\phi)+L_{bf} \qquad \text{dB} \qquad (20)$$

It is to be noted that the basic transmission loss is the main reference figure for the effect of clutter, but it does not provide the contribution of each ray to the overall power budget.

This information is needed to evaluate the effect on interference in the case of use of directional antennas at the transmitter, as discussed in the next chapter.

Therefore, it can be convenient to describe the clutter loss as a vector parameter, $\overrightarrow{l_{cl}}(\theta, \phi)$, providing all the $N_L + 1$ components that contribute to the transmission of power to the receiver.

$$\overrightarrow{l_{cl}}(\theta, \phi) = \left(l_d, l_{Rd} \cdots l_{RN_L}\right) \tag{21}$$

And $l_{cl}(\theta, \phi) = 1/(\frac{1}{l_d} + \frac{1}{l_{Rd}} + \sum_{i=2}^{N_L} \frac{1}{l_{Ri}})$ (see equation (18).

The clutter loss vector parameter in dB is:

$$\overrightarrow{L_{cl}}(\theta, \phi) = \left(L_d, L_{Rd} \cdots L_{RN_L}\right) \quad \text{dB} \tag{22}$$

2.2 Directional antenna case

When the ground transmitter uses a directional antenna, the total power arriving at the antenna of the receiver in space is:

$$p_{RD}(\theta, \phi) = p_t \cdot \left[\frac{g_1}{l_{cld}(\theta,\phi)} + \sum_{i=2}^{N_L} \frac{g_i}{l_{Ri}(\theta,\phi)}\right] \cdot \left(\frac{\lambda}{4\pi d}\right)^2 \quad \text{W} \tag{23}$$

where $g_i > 0$ is the gain in natural units of the transmitting antenna *A* in the direction (θ_i, ϕ_i), $g_i = g(\theta_i, \phi_i)$ with $(\theta, \phi) \equiv (\theta_1, \phi_1)$[7], l_{Ri} is defined in equation (15), $l_{cld} = 1/\left(\frac{1}{l_d} + \frac{1}{l_{Rd}}\right)$ is the total clutter loss of the direct ray and $p_t \cdot g(\theta_i, \phi_i)$ is the effective isotropic radiated power (e.i.r.p.) of the transmitting antenna along direction *i*.

The effective isotropic clutter loss, l_{EIcl}, is defined as the ratio between the power that is received using an omnidirectional antenna without any clutter, $p_t \left(\frac{\lambda}{4\pi d}\right)^2$, and the power that is received using the directional antenna A in presence of clutter and ground reflection, p_{RD}.

$$\frac{p_t}{p_{RD}(\theta,\phi)} \left(\frac{\lambda}{4\pi d}\right)^2 = l_{EIcl}(\theta, \phi) = 1/\left(\frac{g_1}{l_d} + \frac{g_1}{l_{Rd}} + \sum_{i=2}^{N_L} \frac{g_i}{l_{Ri}}\right) \tag{24}$$

As an alternative definition, the effective isotropic clutter and ground loss, l_{EIclg}, is the ratio between the power that is received using the omnidirectional antenna A without any clutter and assuming an ideal perfectly reflective ground, $p_t(g_1 + g_{gd})\left(\frac{\lambda}{4\pi d}\right)^2$ where $g_{gd} = g(-\theta, \phi)$ is the antenna directivity towards the ground (which is one of the components in g_i with $i > 1$), and the power p_{RD} received using the directional antenna A in presence of clutter and ground reflection losses.

$$\frac{p_t \cdot (g_1 + g_{gd})}{p_{RD}(\theta,\phi)} \left(\frac{\lambda}{4\pi d}\right)^2 = l_{EIclg}(\theta, \phi) = \left(g_1 + g_{gd}\right)/\left(\frac{g_1}{l_d} + \frac{g_1}{l_{Rd}} + \sum_{i=2}^{N_L} \frac{g_i}{l_{Ri}}\right) \tag{25}$$

---

[7] The effect of the antenna should be calculated as an integral over all directions. In this expression the integral is replaced by the sum of discrete components as an effect of the use of rays.

By definition

$$l_{EIclg}(\theta, \phi) = \left(g_1 + g_{gd}\right) \cdot l_{EIcl}(\theta, \phi) = g_{ref} \cdot l_{EIcl}(\theta, \phi) \tag{26}$$

with $g_{ref} = \left(g_1 + g_{gd}\right)$.

Using the components of clutter loss, $\overrightarrow{l_{cl}}(\theta, \phi)$ in equation (21), the components of the equivalent antenna clutter loss, $\overrightarrow{l_{Acl}}(\theta, \phi)$ of the selected antenna are:

$$\overrightarrow{l_{Acl}}(\theta, \phi) = \left(\frac{l_d}{g_1}, \frac{l_{R1}}{g_1}, \frac{l_{R2}}{g_2} \cdots \frac{l_{RN_L}}{g_{N_L}}\right) \quad \text{dB} \tag{27}$$

The gain of the antenna for the directions of all launched rays can be represented by vector $\overrightarrow{G_{lray}}$.

$$\overrightarrow{g_{lray}} = (g_1, g_1, g_2 \dots g_{N_L}) \tag{28}$$

Equations (24) and (26) can expressed in dB:

$$\overrightarrow{L_{EIcl}}(\theta, \phi) = -\overrightarrow{G_{lray}} + \overrightarrow{L_{cl}}(\theta, \phi) \quad \text{dB} \tag{29}$$

$$\overrightarrow{L_{EIGcl}}(\theta, \phi) = -\overrightarrow{G_{lray}} + G_{ref} + \overrightarrow{L_{cl}}(\theta, \phi) \quad \text{dB} \tag{30}$$

where $\overrightarrow{G_{lray}} = (G_1, G_1, G_2 \dots G_{N_L})$, $G_{ref} = 10\log_{10}(g_1 + g_{gd})$ and $G_i = 10\log_{10}(g_i)$ dBi are the components of the antenna gain over an isotropic antenna expressed in dBi.

3 Analysis of clutter loss as a stochastic variable

The previous chapters discuss clutter loss as a deterministic parameter, as the result of propagation in a specific environment.

In reality, transmitters on the ground experience a large variety of clutter environments, described by a set of N_e environments $ENV_{cl} = \{e_{cl1}, e_{cl2}, \cdots e_{clN_e}\}$ and therefore the set of rays generated by clutter and arriving at the receiver along a certain direction, RAY_R at frequency f, is a random multidimensional variable resulting from the realisation of the stochastic variables, the environment, $e_{cl} \in ENV_{cl}$ and the position of the transmitter, loc_{gt}.

Hence the total clutter loss l_{cl}, as defined in equation (7) is a stochastic variable described by its cumulative distribution function, conditioned to the reference direction (θ, ϕ), the position of the ground transmitter loc_{gt} and the set of local clutter environments ENV_{cl}:

$$CDF_{cl}\left(x \middle| \theta, \phi, loc_{gt}, ENV_{cl}, f\right) = Pr(l_{cl}(\theta, \phi, f) \leq x | e^*_{cl}) \tag{31}$$

where $x \geq 1/(1 + N_L)$ see equation (18) and e^*_{cl} is the electromagnetic clutter environment defined in equation (8).

One parameter relevant for frequency sharing analysis is the probability of having clutter loss, P_{cl0}, defined as:

$$P_{cl0}\left(\theta, \phi, loc_{gt}, ENV_{cl}\right) = Pr\left(l_{cl} \leq 1 \middle| \theta, \phi, loc_{gt}, ENV_{cl}\right) \tag{32}$$

The expression for total clutter loss can be extended to the case of the components of clutter loss (see equation (21)). In this case the dependence from the position of the receiver and the environment is omitted to simplify the notation.

$$CDF_{cl}(\vec{x}|\theta,\phi) = Pr\left(\overrightarrow{l_{cl}}(\theta,\phi) \leq \vec{x}\right) \quad (33)$$

This description requires the determination of a multidimensional distribution via measurements or simulations that can be a complex task. To simplify the analysis, it can be assumed, as a first approximation, that the clutter loss of the direct ray, is dominant and all the other components due to reflections, $l_{R1} \dots l_{RN_L}$, are mutually independent.

$$Pr\left(l_{Ri} \leq x_i, l_{Rj} \leq x_j\right) = Pr(l_{Ri} \leq x_i) \cdot Pr\left(l_{Rj} \leq x_j\right) \quad (34)$$

with $i \neq j$ and i and j range from 1 to N_L.

The assumption of statistical independence of the two components l_{Ri} and l_{Rj} can be tested using the statistical dependence index, $\chi_{l_{Ri}l_{Rj}}(x_i, x_j)$, and the mutual dependence value $I\left(l_{Ri}; l_{Rj}\right)$[8] :

$$\chi_{l_{Ri}l_{Rj}}(x,y) = \frac{Pr\left(l_{Ri}>x, l_{Rj}>y\right)}{Pr(l_{Ri}>x) \cdot Pr\left(l_{Rj}>y\right)} \quad (35)$$

$$I\left(l_{Ri}; l_{Rj}\right) = \int_{l_{Ri}} \int_{l_{Rj}} Pr\left(l_{Ri} > x, l_{Rj} > y\right) \log_{10}\left[\chi_{l_{Ri}l_{Rj}}(x_i, x_j)\right] dx\, dy : \quad (36)$$

This permits to express the joint distribution of clutter loss due to direct ray and reflected component *i*, using:

$$Pr(l_d \leq x_0, l_{Ri} \leq x_i) = Pr(l_{Ri} \leq x_i | l_{d1} \leq x_0) \cdot Pr(l_d \leq x_0) \quad (37)$$

where $Pr(l_{Ri} > x_i | l_d > x_0)$ is the distribution of the clutter loss due to the reflected component *i* and $Pr(l_d > x_0)$ is the distribution of the clutter loss of the direct ray.

This result can be scaled to the case of the joint distribution of the direct ray and two or more reflected components. To this end, the notation is simplified using $P(\mathrm{x}) \equiv Pr(l \leq x)$, where l is one of the components of the clutter loss.

The joint distribution of l_d, l_{Ri} and l_{Rj} can be written as:

$$P\left(l_d, l_{Ri}, l_{Rj}\right) = P\left(l_{Ri}, l_{Rj} \middle| l_d\right) \cdot P(l_d) \quad (38)$$

In the same way, joint distribution of l_{Ri} and l_{Rj} conditioned to l_d is:

$$P\left(l_{Ri}, l_{Rj} \middle| l_d\right) = P\left(l_{Ri} \middle| l_d, l_{Rj}\right) \cdot P\left(l_d, l_{Rj}\right) \quad (39)$$

Variables l_{Ri} and l_{Rj} are assumed to be independent so:

$$P\left(l_{Ri} \middle| l_d, l_{Rj}\right) = P(l_{Ri} | l_d) \quad (40)$$

---

8 The *complementary cumulative distribution is used for the definition of mutual dependence value I. to put in evidence the statistical effect of low values of clutter loss (n.b. CCDF = 1-CDF).*

Therefore, equation (39) can be rewritten as:

$$P(l_{Ri}, l_{Rj}|l_d) = P(l_{Ri}|l_d) \cdot P(l_d, l_{Rj}) = P(l_{Ri}|l_d) \cdot P(l_{Rj}|l_d) \cdot P(l_d) \quad (41)$$

And equation (38), is:

$$P(l_d, l_{Ri}, l_{Rj}) = P(l_{Ri}|l_d) \cdot P(l_{Rj}|l_d) \cdot P^2(l_d) \quad (42)$$

This expression can be generalized to the case of the joint cumulative distribution of the components of clutter losses generated using N_L rays.

$$Pr(l_{d1} \leq x_0, l_{R1} \leq x_1, .., l_{RN_L} \leq x_{N_L}) = Pr(l_{R1} \leq x_1|l_{d1} \leq x_0) \cdot Pr(l_{R2} \leq x_2|l_{d1} \leq x_0) \; ... \; Pr(l_{RN_L} \leq x_{N_L}|l_{d1} \leq x_0) \cdot Pr^{N_L}(l_{d1} \leq x_0) \quad (43)$$

3.1 Classification of the link according to the line-of-sight condition

It can be useful to perform a classification of the link between the station on earth and the station in space, using the state of the direct link with respect to the clutter environment. To this end, the following categories can be used:

– Non-line-of-sight (NLoS): the direct path between the ground station and station in space is completely obstructed by clutter. This is conventionally set to a value of the loss along the direct path, $L_d > 6$ dB.

– Line-of-sight (LoS): The direct path between earth/ground station and satellite is clear or partially obstructed by clutter. This class can be further split in two sub-classes, using as a reference the knife-edge diffraction model and the loss associated with the 1st Fresnel zone:

  • Fresnel-clear line of sight (FcLoS): The direct path (optical) path is clear and there is no loss along the direct path, $L_d \leq 0$ dB.

  • Fresnel-obstructed line of sight (FoLoS): The direct path (optical) path between is clear and the loss along the direct path is, $0 < L_d \leq 6$ dB.

According to this classification the following probabilities of the line-of-sight conditions can be defined:

– p_{FcLoS}, %: The probability that the direct path (optical) path is in Fresnel-clear line of sight, with. $L_d \leq 0$ dB.

– p_{FoLoS}, %: The probability that the direct path (optical) path is in Fresnel-obstructed line of sight, with $0 < L_d \leq 6$ dB.

– $p_{LoS} = p_{FoLoS} + p_{FcLoS}$, %: Probability of the Line-of-sight (LoS) condition, $L_d \leq 6$ dB.

– $p_{NLoS} = 100 - p_{LoS}$: Probability of the non-line-of-sight (NLoS) condition $L_d > 6$ dB.

Considering these definitions, their relationships and the relevance for interference analyses of the state of the Fresnel-clear line of sight (FcLoS), the use of p_{LoS} and p_{FcLoS} permits a complete classification of the state of the link, using a distribution of p_{FcLoS} conditioned to p_{LoS}:

$$p_{FcLoS} = Pr(FcLoS|LOS) \cdot Pr(LOS) = p_{FcLoS|Los} \cdot p_{LOS} \quad (44)$$

4 Ray launching stochastic methods for clutter loss distribution

The use of Monte-Carlo method of random-draws provides a possible method to assess the distribution of clutter loss.

As discussed before, the clutter loss is the result of a certain environment. Therefore, if the statistical distribution of the elements of the clutter environment $Pr(e_{cl} > x)$, with $e_{cl} \in ENV_{cl}$ is known (e.g. as a result of the survey of a local environment) it can be used to derive a realisation of the environment from a random draw of the probability, P. Then this realisation of the clutter environment can be used by a ray launching algorithm considering N_{RL} rays, with $N_{RL} \geq 1$ and $N_{RL} \leq N_L$ where N_L is the number of all possible rays created by clutter or ground reflections (see equation (2)). This corresponds to assume that the N_{RL} rays selected for ray launching are statistically more relevant for the distribution of clutter loss than all the other rays generated by the clutter environments[9]. This assumption can be verified by analysis of the components of the clutter loss, $\overrightarrow{l_{cl}}(\theta, \phi)$, obtained using ray tracing simulations or measurements.

Figure 4 provides the schematic description of a Ray launching stochastic method.

FIGURE 4

Schematic description of a Ray launching stochastic model (dependency on (θ, ϕ) is omitted) the statistical distribution of clutter can be changed to simulate different environments

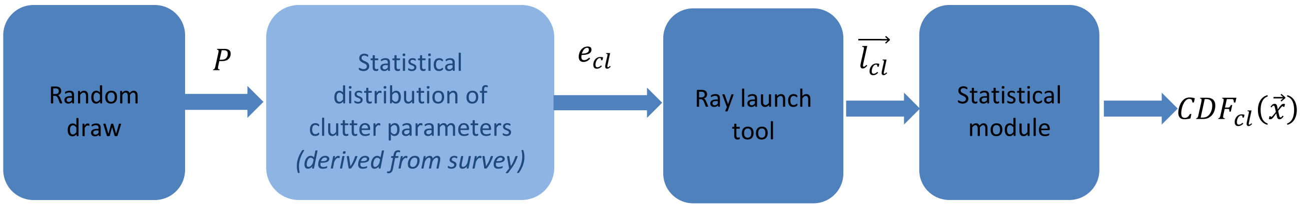

In general, the number of launched rays is limited by assuming that other rays do not contribute significantly, and the stochastic variation is obtained mainly with the simulation of several clutter environments. In this way the computational complexity is reduced significantly and at the same time many samples can be generated permitting to derive statistically significant parameters.

By definition, a ray launching stochastic method can generate the multidimensional distribution of all components of the clutter loss (see equation (24)) that can be simplified (see equation (43)) assuming the statistical independence between reflected components (see equation (34)). This assumption can be verified directly using the stochastic model and the parameters in equations (35) and (36).

In addition, the implementation of ray launching in a stochastic model uses a certain number of EM models for wave propagation (e.g. diffraction, reflection, properties of materials) that needs also to validated using independent methods and data.

Figure 5 provides a baseline description of a possible verification of the assumptions of the ray launching stochastic method.

[9] A parameter is defined as statistically relevant / not relevant when its exclusion from the statistical analysis affects/does not affect the considered statistical parameter more than a predefined threshold.

FIGURE 5

Baseline description for the analysis of the accuracy of the stochastic model using ray tracing or measured data (the superscript * indicates that a parameter is determined in the test campaign)

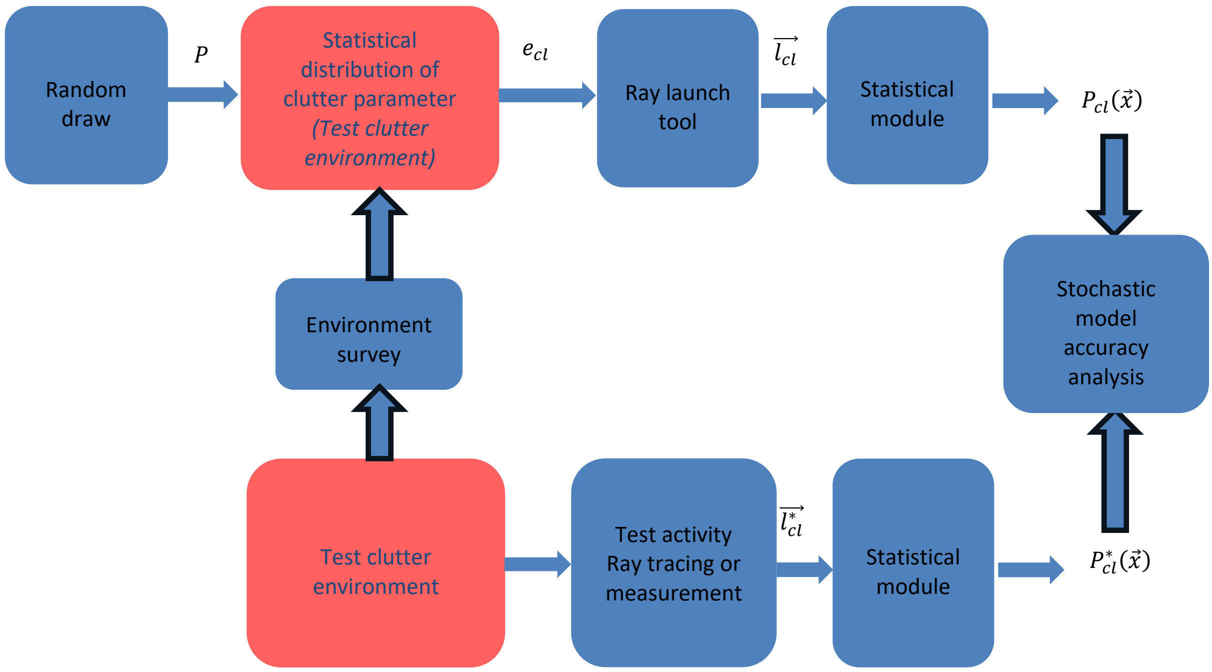

A key aspect of the validation is the statistical representativeness of the distributions of the clutter parameters of the test clutter environment. As the test activity (ray tracing analyses or measurement campaign) could cover an area smaller than the typical size of a city (e.g. from 1 to less than 10 km^2 versus 100 km^2 or more), these distributions could represent few of all the contributions to the distributions of a large area. To this end the test activity should provide also the distributions of the clutter parameters in a larger area containing the area of the test activity to be used by the stochastic model.

The following sections describe in general the stochastic models of Report ITU-R P.2402-0 and Chapter 2 of this Report. An overview comparison of these methods can be found in Annex 3 to this Report.

4.1 Method in Report ITU-R P.2402-0

In this case the parameters of a clutter environment are derived by random draw from the set of distributions of building heights and distances derived from survey points in London (UK) and Melbourne (Australia), here defined as ENV_{cl1}.

In this method, only one ray is launched towards the satellite, so the ray launching simulation considers a single ray at positive elevation angles, i.e. $N_L = 1$.

Each realisation of the random draw generates a clutter scenario with four buildings.

– Buildings 1 and 2 (b1 and b2) are in front of the ground station in the direction of the ray and are one after the other.

– Building 3 is facing buildings 1 and 2 and it is considered only in case of reflections from one of them in case of blocking.

– Building 4 is in front of building 3 (b3) and is considered only for blocking reflections from building 3.

The main characteristics of this stochastic simulation are:

– It considers only the propagation of the ray along the direct path and does not include ground reflections, $\theta \geq 0$.
– The ray tracing considers the direct ray and its eventual reflections by buildings, $N_{RL} = 2$, $RAY_L = \{ray_d\}$ and $RAY_R = \{ray_d, ray_{Rd}\}$.
– The location of the ground transmitter is identified by its height H_s.
– The geometry of the environment and the simulation do not include dependence on azimuth angle[10]. This means (see equation (31)):

$$P_{cl}(x|\theta, ENV_{cl1}) = \int_0^{2\pi} Pr(L_c \leq x|\theta, \phi, ENV_{cl1}) d\,\phi \quad (45)$$

– It includes diffraction loss along the direct path $l_{d1}(\theta)$ by buildings b1 and b2. The combined diffraction loss is calculated assuming knife-edge diffraction for each building and using correction factor derived from the double isolated edges of Recommendation ITU-R P.526.
– It assumes a maximum of two reflections from buildings (i.e. reflections from b1 and b3, b2 and b3, b1 or b2) with no additional diffraction.
– The loss of each reflection depends only on frequency f GHz and is always larger than 8 dB (see equation (15) in Report ITU-R P.2402).
– In this model, there is no relationship between diffraction and reflection losses of a building, therefore the amount of transmitted power is not conserved.
– The clutter loss for each realisation (equation (16) in Report ITU-R P.2402-0) corresponds to total clutter loss l_{cl} of equation (18) (or L_{cl} in dB).

  It is to be noted that, for low values of diffraction losses and one reflection with a minimum loss, L_{cl} can be negative (see Fig. 10 of Report ITU-R P.2402-0).

4.1.1 Use of directional antennas with the method in Report ITU-R P.2402-0

This method launches one ray along the direct path to the satellite identified by direction (θ, ϕ), with θ between 0 and $+\pi/2$.

It is assumed to use an antenna A with a gain pattern $g(\theta, \phi)$ and an antenna boresight direction (θ_b, ϕ_b) with $g(\theta_b, \phi_b) = Max(g(\theta, \phi))$.

The gain of the antenna along the direction of the direct ray is $g_1 = g(\theta - \theta_b, \phi - \phi_b)$.

The effective isotropic clutter loss (see equation (24)) in natural units is:

$$l_{EIcl}(\theta, \phi) = 1/\left(\frac{g_1}{l_d} + \frac{g_1}{l_{Rd}}\right) = \frac{l_{Cld}}{g_1} \quad (46)$$

where $l_{Cld} = 1/\left(\frac{1}{l_d} + \frac{1}{l_{Rd}}\right)$ is the total clutter loss of the ray launched along the direct path.[11]

4.2 Method in Chapter 2 of this Report

This model uses the same distributions of building heights and distances of Report ITU-R P.2402-0, ENV_{cl1} permitting a direct comparison of results. The model was proposed in is described in also in

---

[10] The different random draws are assumed to consider the effect of street direction on a statistical basis for arbitrary azimuth.

[11] For this model the effective isotropic clutter and ground loss, l_{EIclg} (see equation (26)) is not used because it assumes that there is no ray launched towards the ground.

a scientific paper (see Systems. Electronics 2023, 12, 186, https://doi.org/10.3390/electronics12010186).

Summary of the main characteristics of this stochastic model:

– Two rays are launched from the ground transmitter: one along the direct path at elevation angle θ; and one at negative elevation angle $-\theta$ for ground reflections. Therefore, $N_L = 2$ and $RAY_L = \{ray_d, ray_2\}$ with $ray_d \equiv ray_1$.

– The location of the ground transmitter is identified by its height H_s as in Report ITU-R P.2402.

– For every realisation of the clutter environment the azimuth of the incidence angle on the first building is drawn randomly assuming a uniform distribution between 0° and +60°. Considering that negative azimuth angles give the same effect of positive ones this approach is equivalent to simulate buildings of the environment with an orientation ranging between −60° and +60°.

– The ray tracing process considers each launched ray and its eventual reflections by buildings. The set of rays traced up to the receiver is:

$$RAY_R = \{ray_d, ray_{Rd}, ray_2, ray_{R2}\}$$

– The total diffraction loss of each launched ray is calculated by assuming that the effect from the first two buildings along the path is predominant. The combined diffraction loss of these two buildings is calculated assuming knife-edge diffraction and using a correction factor derived from the double isolated edges of Recommendation ITU-R P.526.

– Reflection from the 1st building, if any, using distance to building 1 in ENV_{cl1}. Reflection from b2 is determined using distances between b1 and b2.

– Reflection coefficient is based on physical assumptions.

– It is assumed that the 1st building reflects only the power which is not diffracted (see equation (9) in https://doi.org/10.3390/electronics12010186). This assumption corresponds to conservation of total power along the two paths generated by a ray.

– For each realisation two separate clutter losses (l parameter in equation (12) in https://doi.org/10.3390/electronics12010186) are determined, one for a positive elevation, $l_{cl}(\theta)$ and one for the negative elevation produced by ground reflection $l_{gr} = l_{cl}(-\theta)$. It is to be noted that because of the assumption of conservation of ray power and the separation of statistics for a ray transmitted at positive and negative elevation angles (ground reflection) L_{cl} in dB is always non-negative.

– The statistics of the losses of the direct ray and of the ray at negative elevation angles are calculated separately (see § 6 in Chapter 2). This is done for permitting in a subsequent step, the combination of losses when considering a directional antenna, assuming equiprobability of their values.

4.2.1 Use of directional antennas with the method in Chapter 2 of this Report

This method launches two rays, one towards the satellite along the direction (θ, ϕ) corresponding to the direct path to the satellite, with θ between 0 and $+\pi/2$, and the other towards the ground with angle $-\theta$ and same azimuth angle ϕ.

It is assumed to use an antenna A with a gain pattern $g(\theta, \phi)$ and an antenna boresight direction (θ_b, ϕ_b) with $g(\theta_b, \phi_b) = Max\big(g(\theta, \phi)\big)$.

The gain of the antenna along the directions of the two launched rays are $g_1 = g(\theta - \theta_b)$ and $g_2 = g(-\theta - \theta_b)$.

The effective isotropic clutter loss (see equation (24)) in natural units is:

$$l_{EIcl}(\theta, \phi) = 1/\left(\frac{g_1}{l_d} + \frac{g_1}{l_{Rd}} + \frac{g_2}{l_{R2}}\right) = 1/\left(\frac{g_1}{l_{cld}} + \frac{g_2}{l_{R2}}\right) \quad (47)$$

where $l_{cld} = 1/\left(\frac{1}{l_d} + \frac{1}{l_{Rd}}\right)$ is the total clutter loss of the ray launched along the direct path.

The effective isotropic clutter and ground loss (see equation (26)) in natural units is:

$$l_{EIclg}(\theta, \phi) = (g_1 + g_2)/\left(\frac{g_1}{l_{cld}} + \frac{g_2}{l_{R2}}\right) = (g_1 + g_2) \cdot l_{EIcl}(\theta, \phi) \quad (48)$$

4.3 Univ. of Vigo four ray stochastic method

The University of Vigo clutter loss model for slant paths is a geometric-stochastic model that assumes a transmitter immersed in a built-up environment showing a grid structure (Manhattan). The required inputs are the elevation angle, the transmit antenna height, the street width, the average building length, the distribution of the building heights (a Rayleigh distribution is assumed characterized by its modal value).

For a single elevation, the effect of all possible street orientations and all possible positions of the transmitter in the street are averaged into a single output clutter loss cumulative distribution function.

Rays in the forward direction, in the backward direction and the on to the receiver, or alternatively via ground reflections are power summed at the receiver. Multiple diffraction effects in the forward direction are taken into consideration.

The model can thus be tailored to dense urban or lighter built-up conditions. Additionally, any possible antenna height is possible, above or below the surrounding rooftops, thus encompassing both macro- and micro-cellular base stations. The low antenna heights can be used to model user terminals deep within the built-up surroundings.

4.3.1 Use of directional antennas with the UVigo four ray method

This method launches four rays, ray_1 towards the satellite along the direction (θ, ϕ) corresponding to the direct path to the satellite, with θ between 0 and +π/2, ray_2 towards the ground with angle $-\theta$ and same azimuth angle ϕ, ray_3 with opposite azimuth angle $\phi - \pi$, and positive elevation angle θ (reflected by the rear building) and ray_4 towards the ground with angle $-\theta$ and apposite azimuth angle $\phi - \pi$ (reflected by the rear building).

It is assumed to use an antenna A with a gain pattern $g(\theta, \phi)$ and an antenna boresight direction (θ_b, ϕ_b) with $g(\theta_b, \phi_b) = Max\big(g(\theta, \phi)\big)$. The direction (θ, ϕ) corresponds to the direct path to the satellite, with θ between 0 and +π/2. The gain of the antenna along the directions of the four rays launched in the UVigo model, $ray_1, ray_2, ray_3, ray_4$ are:

$$g_1 = g(\theta - \theta_b, \phi - \phi_b)$$

$$g_2 = g(-\theta - \theta_b, \phi - \phi_b)$$

$$g_3 = g(\theta - \theta_b, \phi - \pi - \phi_b)$$

$$g_4 = g(-\theta - \theta_b, \phi - \pi - \phi_b)$$

l_{Rx} is the clutter loss in natural units of the rays R_x received by the satellite (i.e. R_d, R_{Rd}, R_{R2}, R_{R3} and R_{R4})[12].

The effective isotropic clutter loss (see equation (24)) in natural units is:

$$l_{EIcl}(\theta,\phi) = 1/\left(\frac{g_1}{l_d}+\frac{g_1}{l_{Rd}}+\frac{g_2}{l_{R2}}+\frac{g_3}{l_{R3}}+\frac{g_4}{l_{R4}}\right) = 1/\left(\frac{g_1}{l_{Cld}}+\frac{g_2}{l_{R2}}+\frac{g_3}{l_{R3}}+\frac{g_4}{l_{R4}}\right) \quad (49)$$

where $l_{Cld} = 1/\left(\frac{1}{l_d}+\frac{1}{l_{Rd}}\right)$ is the total clutter loss of the ray launched along the direct path.

The effective isotropic clutter and ground loss (see equation (26)) in natural units is:

$$l_{EIclg}(\theta,\phi) = (g_1+g_2)/\left(\frac{g_1}{l_{Cld}}+\frac{g_2}{l_{R2}}+\frac{g_3}{l_{R3}}+\frac{g_4}{l_{R4}}\right) = (g_1+g_2)\cdot l_{EIcl}(\theta,\phi) \quad (50)$$

5 Ray-tracing stochastic model for clutter loss distribution

5.1 Description of the models used for Recommendation ITU-R P.2108

This paragraph provides a summary of the studies done by Study Group 3 to develop the method provided in Recommendation ITU-R P.2108, Annex 1, § 3.3 "Earth-space and Aeronautical statistical model".

The model is based on the models for the probability of line-of-sight (LoS) conditions of the direct link (as defined in § 3.1) and for the distribution of clutter loss in the case of an isotropic antenna, L_{cl}. Both models were derived using ray-tracing simulations for various reference scenarios, described in Annex 5.

5.1.1 Model for the probability of line-of-sight conditions

The model for the probability of LOS, p_{LOS}, and its associated probability of FcLOS when the link is Fresnel clear LOS conditions, $p_{FcLoS|Los}$ was derived by running ray tracing simulations on three scenarios and validated using an additional one. These scenarios are described in Annex 5, paragraph A.

In these scenarios about 603 stations in space were uniformly distributed over the ground zone in a dome up to a height of about 20 km. About 1 000 earth/ground station were randomly distributed on the ground and their height was uniformly distributed between 1 m and the value of the 90 percentile of the distribution of building heights of the specific scenario. The area of the ground zone used for the simulation was reduced by using a border exclusion zone of about 150 m to reduce the effect of the boundaries of the ground zone map on the results. The simulations were performed for frequencies ranging from 0.7 to 15 GHz. For each scenario p_{LOS} and $p_{FcLoS|Los}$ were calculated for a range of heights of the earth/ground stations and elevation angles between 0 and 90 degrees.

The results for three simulation scenarios, London UK, Leichardt Sydney Australia and Shibuya, Tokyo Japan were used to determine the parameters of the model, while validation was done using Paris, France, as an independent scenario.

The resulting model is provided in Recommendation ITU-R P.2108-2, Annex 1, § 3.3.2 equations (7) to (11), and provides p_{LOS} and p_{FcLoS} using as input: frequency (not needed for p_{LoS}), elevation angle,

---

[12] In this notation the capital R in the subscript of the received ray x, R_{Rx}, indicates that it has been generated by reflection from clutter and/or ground.

earth/ground station height and median clutter height, which is used to differentiate between three conventional scenarios (low, mid and high-rise).

5.1.2 Model for distribution of clutter loss for an isotropic antenna

This model was derived using CloudRT, a high-performance and cloud-based 3D ray tracer, for three scenarios, described in Annex 5, paragraph B. The space stations were distributed in a dome over the ground zone up to a height of 20 km and at elevation angles ranging from 10 to 90 degrees with 10 degrees intervals and azimuth angles from 0 to 360 degrees with 45 degrees intervals. The simulations were performed for frequencies 0.5, 1, 1.5, 2, 3, 4, 5, 6, 7, 8 and 9 GHz using a 1st order reflection, the Deygout model to account for diffraction from multiple edges and EM property of materials derived from Recommendations ITU-R P.2040-3, ITU-R P.527-6, and ITU-R P.833-10. The reflection model accounted for the roughness of the surfaces using the Rayleigh roughness model and a characteristic roughness height of 0.1 m.

The model was derived by fitting on the results of ray-tracing simulations and is provided in Annex 1, § 3.3.2 equations (12) to (15) of Recommendation ITU-R P.2108-2, and it is a piecewise function based on three separate distribution functions for the probability ranges from 0 to p_{FcLoS} (for Fresnel-clear line of sight); from p_{FcLoS} to p_{LoS} (for Fresnel-obstructed line of sight) and from p_{LoS} to 100% (for NLoS).

– The distribution function for the condition of Fresnel-clear line of sight, equation (15), uses a double exponential model with input p_{FcLoS}.

– The distribution function for the Fresnel-obstructed line of sight condition, equation (14), is a uniform distribution ranging from 0 to 6 dB, the conventional upper value for FoLoS condition.

– The distribution function conditioned to NLoS, equation (12b), is based on a normal distribution, with a minimum value of 6 dB and it depends on the elevation angle and frequency.

5.2 Use of ray-tracing statistical model with directional antennas

The spatial characteristics of the link between a station on the ground using a directional antenna and a satellite or aircraft station with a Fresnel clear line-of-sight (FcLoS) between the two stations, could be modelled, as a first order approximation, using a two-rays model. The first ray aligns with the geometrically shortest path between the transmitter and receiver along the direction identified by (θ_1, φ_1), where φ_1 is the azimuth angle from the earth/ground station to the elevated station, and θ_1 is the elevation angle from the earth/ground station to the elevated station. The direction of the second path, (θ_2, φ_2), with $\varphi_2 = \varphi_1$ and $\theta_2 = -\theta_1$.

In such FcLoS cases, the clutter loss along the direct path $L_{cld}(\theta, \varphi)$ is assumed to be equal to 0 dB and the additional clutter loss of the secondary $L_{clg}(-\theta, \varphi)$ path can be modelled as $\beta' = \max(0, \beta)$, where $\beta \sim N(17,6)$ dB, where $N(m, \sigma)$ is a Gaussian distribution function with mean value m and standard deviation σ. The parameters of the model are derived from measurements.

Following this approach, the interference or received power could be calculated with the formula provided in Annex 2, paragraph B.

CHAPTER 2

Stochastic model for clutter loss including direct path and ground reflections

1 Introduction

This chapter describes methods for predicting what is often called "clutter loss". In the context of radio, the term "clutter" may have originated with the development of radar, since unwanted returns on a radar screen are also termed clutter. In general propagation modelling, clutter loss means losses due to propagation within objects which are on the ground but which are not the ground itself. In this context "clutter" means buildings.

This Report covers only losses due to urban or suburban clutter. Within this classification, any man-made objects can be included, particularly those of sizes comparable to buildings, such as bridges.

The term clutter loss also implies a certain type of radio path, characterized by having:

a) one station embedded within clutter, such as below roof level in an urban area;

b) the radio path extends beyond the influence of clutter.

This concept can apply to:

i) a path to an aeronautical or high-altitude platform station;

ii) a path to a station in space.

In all these cases the clutter loss at the station embedded within the clutter can be evaluated as an end-correction, to be added to losses calculated using other models applying to the whole length of the path.

The building statistics used to create the clutter loss cumulative distributions are given in § 7 and [provided/available] as digital product [integral/supplemental] to this Report.

The results of the stochastic model for a range of frequencies, elevation angles and heights of the transmitter are [provided/available] as digital product [integral/supplemental] to this Report

2 Urban clutter

Urban clutter varies greatly in its materials and geometry, and thus its propensity for causing obstruction losses. Another characteristic of urban clutter is that many buildings have reflective surfaces which in some cases can support specula reflection with low loss. It is possible for clutter loss to be negative when multiple rays are taken into account.

A long-term difficulty in modelling variability of clutter loss concerns the classification of urbanisation. Reliance has often been placed on qualitative descriptions such as "dense urban", with quantitative metrics often limited to typical building heights. Such classification fails to capture details relevant to propagation, such as the difference between street canyons with fairly continuous lines of buildings, and more open areas with perhaps taller but more separated buildings.

The sketches in Fig. 6 illustrate these cases. Paths from antennas within the street canyons in a) are obstructed except in the directions nearly parallel to the streets. In Fig. 6 b), more paths exist between buildings, and even when a building causes obstruction the diffraction loss to one side might be lower than diffraction over the roof. Thus, even if the buildings in Fig. 6 b) are higher than in Fig. 6 a), diffraction losses will not necessarily be greater, and reflections may have more effect in reducing overall losses. It is thus to be expected that the statistics of urban clutter loss can differ substantially between these two types of urban area.

FIGURE 6

Urban areas formed of street canyons or separate building blocks

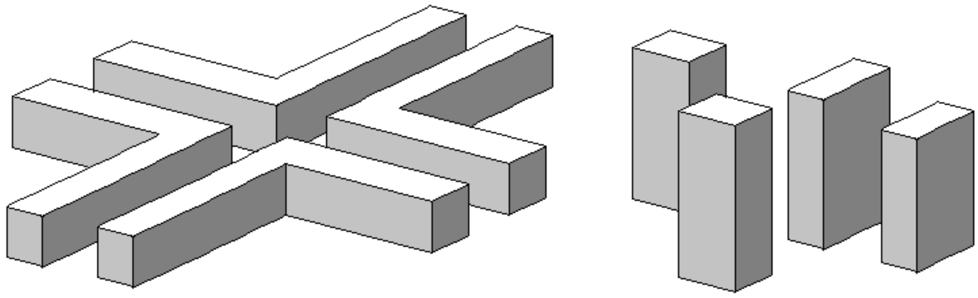

While the Report refers to urban clutter, it is believed that it is equally applicable to any built-up area e.g. suburban clutter.

3 General form of a statistical urban clutter-loss model

A statistical model for clutter loss in urban environments is most suitable for scenarios with an area deployment of stations within a particular type of urban area. The model described here has the following general form:

a) A specific example of a general type of urban environment is characterised by compiling cumulative distributions of horizontal distance and building heights. These distributions capture the characteristics of the area with respect to street width, fraction of ground covered, building heights, and changes in ground level. Collectively these statistics are referred to as the template for the area actually surveyed and can be representative of other urban areas judged to be sufficiently similar.

b) The statistics comprising a template are collected for a number of survey points within the specific example of urbanisation. The horizontal positions of these survey points should be typical of the locations of the expected area deployment of station within the clutter. Assuming that an area-coverage system is in view, stations might be on building faces, above the kerbs along the edges of pavements (sidewalks), etc. Another distinction is whether each station to be deployed is intended to have the largest practicable coverage area, or to cover a smaller area in order to maximise traffic density. If different deployment strategies are expected in different cases, correspondingly different templates are required for the same type of urbanisation.

c) The location of survey points has no connection with the expected height at which stations will be deployed. Different templates do not have to be compiled for different station heights.

d) A stochastic process evaluates diffraction and reflection losses based on distances and heights generated randomly from the template statistics, the building or ground material, the type of polarization (transverse electric (TE) or transverse magnetic (TM)) and the angle of incidence. The resulting clutter loss is thus also random, but all such results for the same template, station height above ground, path elevation angle, angle of incidence, type of polarization and frequency are equally probable. The considered building and ground material could follow the template statistic or be equally probable. The model is run a sufficient number of times to compile a cumulative distribution of clutter loss to the required statistical certainty.

e) The stochastic process takes only horizontal distances and vertical heights into account. There is no concept of azimuth within this part of the method but the orientation of the ray in the horizontal plane with respect to the direction orthogonal to the building surface is assumed to be random in the range between −60 degrees and +60 degrees The cumulative distribution of loss compiled from repeated use of the process will take into account the effect of street direction on a statistical basis for arbitrary path azimuths. The method is not able to predict the effect of street orientation relative to path direction.

f) The cumulative distributions given by the model can be used directly within a Monte Carlo simulation. Each run of the simulation should generate a new random value for percentage locations p_L with $0\% \leq p_L < 100\%$ from which the model will give a corresponding value of clutter loss for the apparent path elevation angle to be added to the other losses for the path. The effect of the random but equi-probable clutter losses on the ensemble of paths will approximate to the physical paths under consideration, the approximation improving with greater number of path calculations.

g) Because building penetration is not taken into account, the method is not suitable for frequencies at which transmission through building might be significant. Up to about 1 GHz transmission losses through many buildings can be low. The reflection loss is anyway calculated through an electromagnetic simulation considering the interface of various materials up to a frequency of about 100 GHz (10 GHz for some materials). The transition range over which most buildings become effectively opaque to radio is estimated as from 1 GHz to 10 GHz. The statistical method here is suitable for the frequency range between 1 and 10 GHz but could be applicable with reduced accuracy up to 100 GHz.

4 Assembling a template

The urban statistics required by the propagation model consist of probability distributions of horizontal distances and building heights. The following sub-sections give details of the process of compiling them.

4.1 The use of representative survey points

Cumulative probability distributions are compiled for a number of survey points representative of the expected deployment of station locations within the area. Survey points might be placed along street centre-lines, the curb lines or edges of pavements (sidewalks), or on building faces, according to the expected deployment of stations to be represented. An appropriate choice should also be made as to whether stations will typically be installed at street intersections for maximum area coverage in several directions or avoiding intersections to increase isolation between cells.

The plan view in Fig. 7 illustrates the general method. The altitude of ground level at each survey point above sea level A_s (m) is recorded. Then for each horizontal radial at 10-degree intervals, the following are recorded:

a) the horizontal distance D_{b1} (m) to the first building travelling outwards from the survey point;

b) the roof altitude above sea level A_b (m) above the point where the radial meets the building face;

c) the additional horizontal distance D_{b12} (m) to the second building encountered along the same radial.

The two distances are shown on one of the radials in Fig. 7, where for clarity the two buildings involved are not shaded. The other radials are in red and stop where the second building is encountered. Some radials do not encounter a second building within the diagram. The search distance for either a first or a second building is limited to 1 000 m. If no building is encountered within the first 1 000 m, D_{b1} and D_{b12} are both set to 500 m, and A_{b1} is set to terrain height at 500 m distance. If one building is encountered within the first 1 km but not a second, the total distance to the second, D_{b2}, is set to 1 000 m. Although these limits are arbitrary, the corresponding entry for the radial concerned appropriately represents a direction with little obstruction.

FIGURE 7

Compiling urban statistics

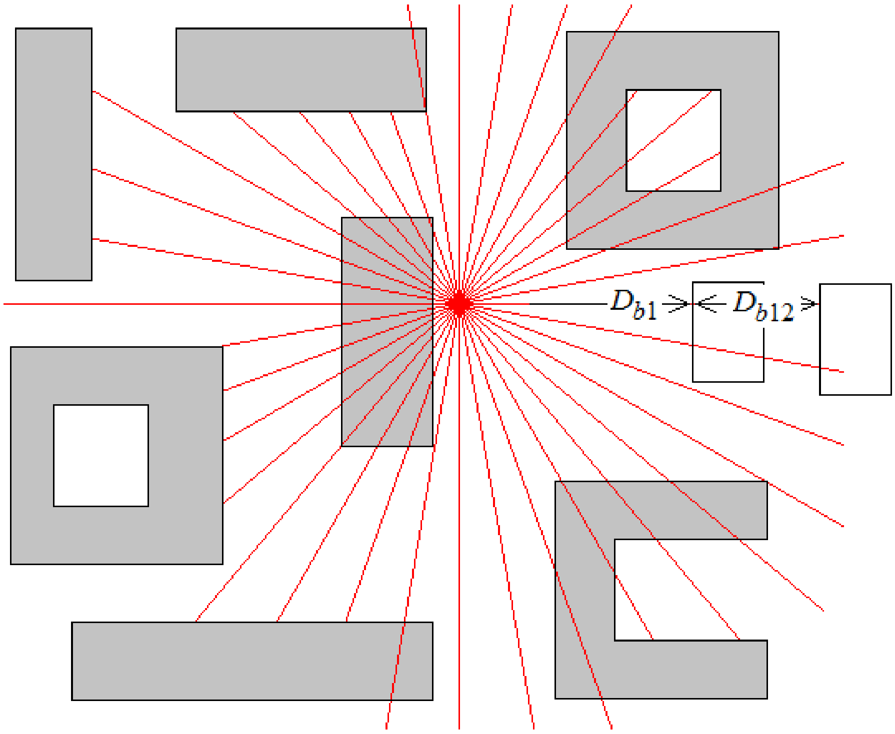

The above process should not be confused with radio-wave propagation modelling, such as ray tracing. The objective is to characterise urban geometry. There is no consideration of, for instance, the width of Fresnel zones. The criterion for a radial encountering a building should be interpreted exactly, however small the margin either way.

Figure 8 illustrates the relationship between roof altitude A_b and building height H_b for a given radial from a survey point to building 1. The heights of ground level at the survey point A_s, and of the building roof A_b, are both altitudes above sea level (m asl). The building height H_b is given by:

$$H_b = A_b - A_s \quad \text{(m)} \tag{51}$$

FIGURE 8

Altitude of building roof and building height

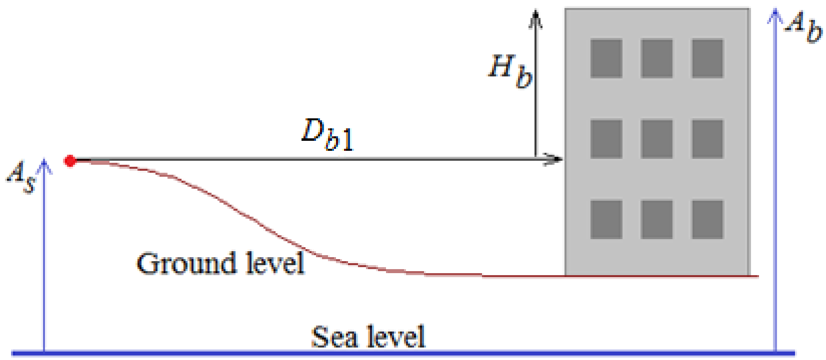

The following points apply to the above urban statistics:

1) It is intended that each roof altitude is recorded close to the roof edge above where the radial meets the external building wall. Consideration should not be given as to whether a different part of the same roof is higher, since: (*i*) it would introduce a subjective process; (*ii*) the ray elevation angle is unknown at this stage; (*iii*) the building height information will be used for both diffraction and reflection which require different treatments, (*iv*) the association which exists between a distance and a height along a given survey radial is discarded in subsequent processing.

2) The second building may be part of the first, as shown for some radials in Fig. 7. The criterion for a second building is that the ray travels over un-built-on ground before reaching it. This is, as in a), a readily interpreted objective condition intended to assist in making urban statistics reproducible.

3) The propagation part of the model could use a second height distribution for the height of the second building, but in various surveys it has been found that, with the criterion in b), a distribution of second heights is so similar to the distribution of first heights that it is not worth compiling the second-building heights.

4) The definition of building height allows changes of ground level within the urban area to be captured. This means that the two distributions characterise not only the nature of the urbanisation itself but also the extent to which the buildings stand on hilly ground.

5) Recording building heights on a per-radial basis, as opposed to one height for each building, tends to weight height probabilities according to building width. This is a desirable feature in view of how the distributions are used.

4.2 Obtaining the distance and altitude data

Any survey method can be used to compile values for A_s, D_{b1}, A_{b1}, and D_{b12} described in § 4.1. The two altitudes (A_s and A_{b1}) are only intermediate values; if appropriate the survey can directly compile building heights relative to ground level at the survey point, H_b. Working units do not need to be mandated, although the following descriptions assume that both distances and heights are in metres.

Examples of sources of the required urban statistics are:

a) direct surveying;

b) large-scale digital maps with building heights;

c) three-dimension model of an urban area derived from LIDAR or stereo photography.

4.3 Conversion to cumulative distributions

The values of D_{b1} D_{b12} H_b collected for all radials at a number of survey points are now treated as three sets of data, with no further association with the survey points or radials from which they were derived.

The three sets of values are used to compile three cumulative distributions.

The distributions of both distances and heights are found to depart considerably from the normal distribution, with large positive skew. The statistics used to represent a typical urban area are thus specific cumulative distributions compiled from the three sets of values for D_{b1} D_{b12} and H_b. No use is made of the means and standard deviations of these distributions.

The statistics are also compiled as population distributions rather than sample distributions. This has the effect that a value extracted from the distribution for any probability will not be less than the lowest value or higher than the highest value.

The data are used to compile three histograms which can be in the form of:

A vector of distances or roof heights:

$$\vec{X} = \{x_1, x_2, \cdots x_N\} \quad \text{(m)} \tag{52a}$$

A corresponding vector of counts:

$$\vec{C} = \{c_1, c_2, \cdots c_N\} \tag{52b}$$

The values in $\vec{X}$ are in ascending order from the lowest value to the highest value. For the sample results presented in § 4 the distance and height values were rounded to the nearest metre. For most locations it is thought that this provides sufficient resolution, although the method can readily be adopted for smaller intervals.

The counts in $\vec{C}$ are the number of occurrences of each value of x. Thus $\vec{X}$ and $\vec{C}$ constitute a histogram.

The corresponding cumulative distribution is compiled by assigning:

$$\vec{P} = \{p_1, p_2, \cdots\} = \left\{\frac{c_1}{C}, \frac{c_1+c_2}{C}, \frac{c_1+c_2+c_3}{C}, \cdots\right\} \tag{53}$$

where:

$$C = \sum_{n=1}^{N} c_n \tag{53a}$$

The value from a vector of distances or heights $\vec{X}$ not exceeded for a given probability p is given by a function Q defined as:

$$Q(\vec{X}, \vec{P}, P) = x_n \tag{54}$$

where n is the highest index for which $p_n \le P$, unless $P \le p_1$ in which case $n = 1$. With these conditions, function Q returns only observed values.

It is noted that with the foregoing expression, the number of elements in $\vec{P}$ is the same as in $\vec{X}$, not one greater. This is the effect of values in $\vec{X}$ being rounded to the nearest metre, and thus the concept of bin width being not applicable.

4.4 Distributions forming a template

Following the procedures described in § 4.3, a template consists of:

a) Vector of distance to first building $\overrightarrow{D_{b1}}$ and corresponding probabilities $\overrightarrow{P_{db1}}$.

b) Vector of distance from first to second building $\overrightarrow{D_{b12}}$ and corresponding probabilities $\overrightarrow{P_{db12}}$.

c) Vector of building height $\overrightarrow{H_b}$ and corresponding probabilities $\overrightarrow{P_{hb}}$.

4.5 Random value from a cumulative distribution

In the propagation model, random values of distances and heights are obtained by generating a uniformly-distributed random probability P in the range $0 \le P < 1$ and using function Q defined by equation (54) to obtain the required value.

5 The stochastic model

The stochastic part of the method calculates the clutter loss for a ray leaving a station located below roof level in an urban area. Random numbers are used to extract building distances and heights from the template which represents the characteristics of the area. These random dimensions define the geometry in a hypothetical vertical plane. There is no concept of azimuth within the geometry but the orientation of the ray in the horizontal plane with respect to the direction orthogonal to the building surface is assumed to be random in the range between −60 degrees and +60 degrees.

Repeated calculations will produce different but equally-probable clutter losses. The calculation must be performed a sufficiently large number of times to obtain the statistical distribution of clutter losses for arbitrary station locations. The repetition of the calculation can be one element of a larger-scale simulation.

5.1 Inputs

A multiple run of calculations to compile clutter-loss statistics requires the following inputs:

a) the statistical characterisation of the representative urban area, as described in § 4 above; i.e. distributions of building heights, distance from of first building from survey point, distance of second building from front of first building;

b) station height above ground level H_s (m);

c) path elevation angle θ (degrees);

d) frequency (GHz), between 1 and 10 GHz (and, with reduced accuracy, up to 100 GHz);

e) ground and building materials for the reflection;

f) polarization.

If wished, station heights above ground can be defined by a probability distribution. This would be appropriate when a range of heights is expected in a planned future deployment.

5.2 Model overview

Figure 9 gives an overview of the stochastic model. The blue ray leaving the station at a given positive elevation angle passes over buildings B_1, B_2, B_{d3}… and B_{dN} (the subscript 'd' is used to identify the diffracting buildings which are different from the reflecting buildings introduced below) with an associated diffraction loss (the knife-edge model is used) which takes into account only buildings B_1 and B_2. This ray, ray 1, always exists, although it may have a high loss. A reflected ray, red ray 2, is originated when the blue ray leaving the station intercepts a building either B_1 below its roof height, or if not, intercepts B_2 below its roof height. If there is a reflected ray, the first reflection will be from either B_1 or B_2, and then all the other possible reflections by buildings B_{r3}, B_{r4}, …, B_{rK} (the subscript 'r' is used to identify the reflecting buildings which are different from the diffracting building mentioned above) before the ray reaches the satellite, are considered. The overall loss of this reflected ray takes into account also the effects of the buildings B_{rd1} and B_{rd2} along the path of the reflected ray (the subscript 'rd' is used to identify the diffracting buildings after reflection): all reflection losses and the diffraction losses are multiplied in natural units.

The two diffracted and reflected rays (the green and red rays) are combined when they are both above all buildings and are travelling towards the satellite. The power radiated from the base station is split when the transmitted blue ray is reflected by the first or second reflecting building B_J, where J = 1 or 2, and proportionally to the diffraction loss (in natural unit) of B_J. By considering the received (interfering) power at the satellite, p_{sat}, it is possible to calculate the overall clutter loss. In fact:

$$p_{\text{sat}} = p_{1,\text{sat}} + p_{2,\text{sat}} = p_t\left(\frac{1}{l_{1,D}} + \frac{1}{l_{1,D,J-1}} \cdot \left(1 - \frac{1}{l_{1,D,J}}\right) \cdot \frac{1}{l_{2,R,J}} \cdot \frac{1}{l_{2,R,r3}} \cdot \ldots \cdot \frac{1}{l_{2,R,rK}} \cdot \ldots \cdot \frac{1}{l_{2,D}}\right) \quad (55)$$

where:

$p_{1,sat}$ (W): received power associated to the ray 1

$p_{2,sat}$ (W): received power associated to the ray 2

p_t : base station radiated power

$l_{1,D}$: total diffraction loss of ray 1 (the diffracted ray)

$l_{2,D}$: total diffraction loss of ray 2 (the reflected ray)

$l_{1,D,J-1}$ is equal to 1 if J=1 and equal to the diffraction loss due to B1 $l_{1,D,1}$ if J = 2

$l_{2,R,r\#}$: reflection loss of ray 2 due to the building $B_{r\#}$.

The overall clutter loss, l_{cl}, in natural unit, is given by:

$$\frac{1}{l_{cl}} = \frac{p_{\text{sat}}}{p_{\text{t}}} = \left(\frac{1}{l_{1,D}} + \frac{1}{l_{1,D,J-1}} \cdot \left(1 - \frac{1}{l_{1,D,J}}\right) \cdot \frac{1}{l_{2,R,J}} \cdot \frac{1}{l_{2,R,r3}} \cdot \ldots \cdot \frac{1}{l_{2,R,rK}} \cdot \ldots \cdot \frac{1}{l_{2,D}}\right) \quad (56)$$

The clutter loss L_{cl} is then calculated in dB:

$$L_{cl} = 10 \cdot \log_{10} cl \quad \text{(dB)} \quad (57)$$

Diffraction losses for two buildings are calculated separately. The total diffraction losses of ray 1 and ray 2, $l_{1,D}$ and $l_{2,D}$ are calculated by considering the two largest diffraction losses due to buildings along their path, $l_{\text{i},D1}$ and $l_{\text{i},D2}$, with i =1 or 2, as though the other does not exist, and their losses are then combined to give the overall diffraction loss with a correction taking account of their separation, similar in principle to the methods for two isolated edges in Recommendation ITU-R P.526:

$$l_{i,D} = \left(l_{i,D1} + l_{\text{i},D2}\right)^{\frac{1+L_{i,D1}+L_{i,D2}}{2+L_{i,D1}+L_{i,D2}}} \quad (58)$$

where $L_{i,D1} = 10 \cdot \log_{10} l_{i,D1}$ and $L_{i,D2} = 10 \cdot \log_{10} l_{i,D2}$.

The method considers also the rays with negative elevation angles (radiated below the horizon) which are reflected by the ground. Of course, after ground reflection, the ray acquires a positive elevation angle (see Fig. 9).

If there is no reflection from B1 or B2, only the diffracted ray, represented by the green arrow in Fig. 9, is considered.

FIGURE 9

Overview of propagation model

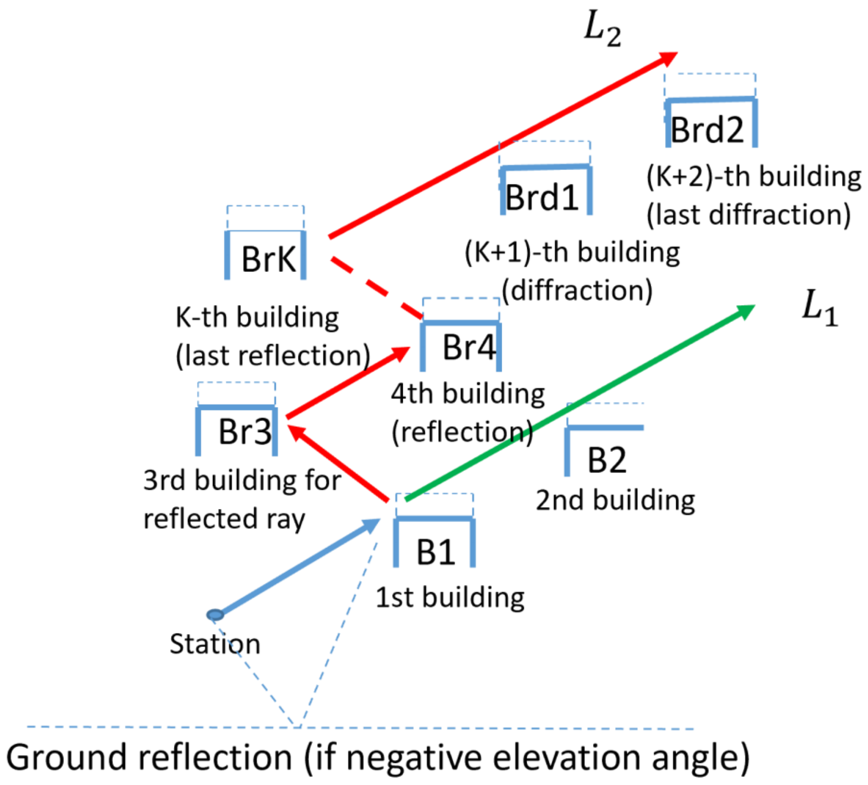

5.3 Obtaining the propagation geometry

The horizontal distances and vertical building heights required to evaluate propagation effects are obtained from the template distributions as follows.

5.3.1 Horizontal distances

The horizontal distance from the station to building 1 is obtained as:

$$D_{b1} = \mathrm{Q}\left(\overrightarrow{D_{b1}}, \overrightarrow{P_{db1}}, P\right) \quad \text{(m)} \tag{59}$$

The horizontal distance from the building 1 to building 2 is obtained as:

$$D_{b12} = \mathrm{Q}\left(\overrightarrow{D_{b12}}, \overrightarrow{P_{db12}}, P\right) \quad \text{(m)} \tag{60}$$

where in both equations (59) and (60) P is a new random number with $0 \leq P < 1$, and function Q is defined by equation (4). The same procedure is applied to calculate the horizontal distance between buildings B_{di} and $B_{d(i+1)}$, with $i = 3, \ldots,$ M-1, and between buildings B_{rdi} and $B_{rd(i+1)}$, with $i = 1, \ldots,$ P-1.

The horizontal distance from the station to building 2 is given by:

$$D_{b2} = D_{b1} + D_{b12} \quad \text{(m)} \tag{61}$$

For the reflection model, all the incremental horizontal distances between buildings B_{ri}, with $i = 3, \ldots, K-1$, are given by:

$$D_{rnm} = \mathrm{Q}\left(\overrightarrow{D_{b1}}, \overrightarrow{P_{db1}}, P\right) \tag{62}$$

and where in each case P is a uniformly distributed random number with $0 \leq P < 1$.

5.3.2 Roof heights

For reflection and diffraction, the roof height of all buildings, above the station, is obtained as:

$$H_b = \mathrm{Q}\left(\overrightarrow{H_b}, \overrightarrow{P_{hb}}, P\right) - H_s \quad \text{(m)} \tag{63}$$

where:

P is a uniformly distributed random number in each case with $0 \leq P < 1$.

5.3.3 Ray heights above the station

The height above the station at which a ray, leaving point x with an elevation angle θ, arrives at building y can be written as a function H_{ray}:

$$H_{ray}\left(H_{rsx}, D_{xy}\right) = H_{rsx} + D_{xy}\tan(\theta) \quad \text{(m)} \tag{64}$$

where:

H_{rsx} : height above the ground at a starting point x where $x = 0$ to indicate the station, and 1 to N to indicate either a building or the point on ground where the ray is reflected.; In case of reflection from ground, for negative elevation angles, H_{rsx}=-$H_{rs(x-1)}$ with $x \geq 1$

D_{xy} : horizontal distance from x to y. If x is a point where the ray is reflected by ground when the elevation angle is negative, D_{xy}=$D_{(x-1)y}$, with $x \geq 1$.

Ray heights are calculated as needed by the diffraction and reflection models.

5.4 Diffraction loss

Diffraction losses for each building impairing a ray are calculated as though any other building does not exist, and the losses of the first two building that diffract the ray are then summed in dB.

The knife-edge model proposed by Recommendation ITU-R P.526-15 is employed: each building is treated as though a knife-edge, for which diffraction loss is given as a function J of a dimensionless parameter ν according to:

$$J(\nu) = \begin{cases} 6.9 + 20\log_{10}\left[\sqrt{(\nu-0.1)^2+1} + \nu - 0.1\right] & \text{if } \nu > -0.78 \\ 0 & \text{otherwise} \end{cases} \quad \text{(dB)} \tag{65}$$

The knife-edge diffraction loss, in natural units, is given by:

$$l_{d1} = 10^{-J(\nu)/10} \tag{66}$$

where:

$$\nu = k\sqrt{\frac{2}{\lambda D_k}} \tag{67}$$

where λ is the wavelength, D_k represents the distance between the base station and the nearest top vertex of the considered building, and k is the distance between the straight line of the ray and the vertex.

The trigonometric analysis allows to obtain the absolute value of k from the elevation angle θ, the distance D_A between the base station and the building A and z, which is the height difference between the base station H_S and the building H_A, and it contains also the information on the mutual position between the base station and the building A (i.e. whether if the building is higher than the base station or not).

FIGURE 10

Possible diffraction scenarios

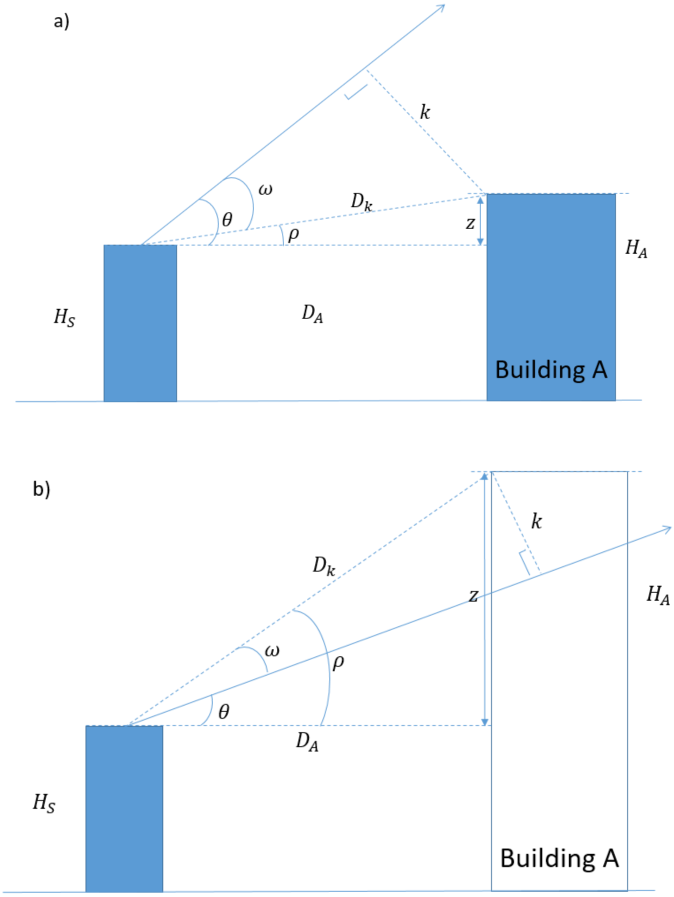

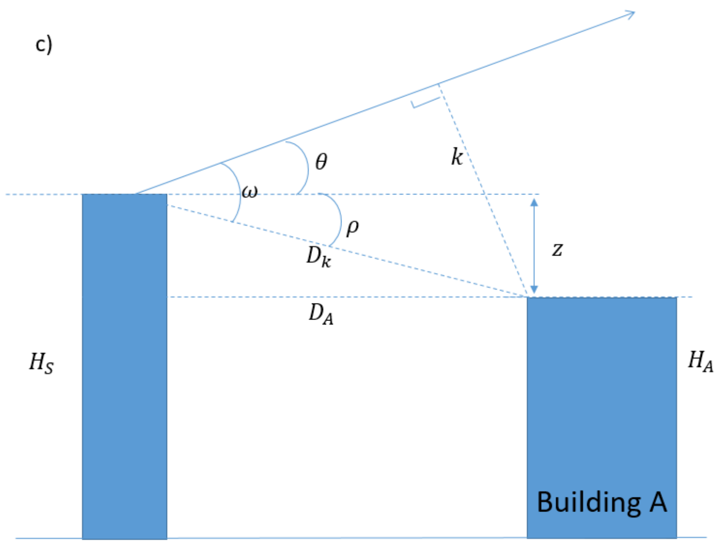

In more detail, three possible specific cases can occur, as depicted in Fig. 10: for the situation represented in Fig. 10.a), the base station is lower than building A, which is overpassed by the launched ray. Thus, the parameters k and D_k are:

$$k = -D_k \sin(\omega) \tag{68}$$

$$D_k = \sqrt{{D_A}^2 + z^2} \tag{69}$$

where D_A is the sum of all the incremental distances from the base station to the building A, extracted for each building as described in § 5.4, z represents the absolute value of the difference between the base station height and the building one ($z = |H_A - H_{BS}|$) and the angle ω is given by:

$$\omega = \theta - \rho \tag{70}$$

where θ is the elevation angle and ρ the angle between the horizontal plane and the line which connects the top of the building to the base station, obtained as $\rho = \cos^{-1}(\frac{D_A}{D_k})$.

The same trigonometric principles are used in the case of Fig. 10 b), where building A is higher than the base station, but the ray hits the building. With respect to the situation presented in Fig. 10 a), nothing changes about the calculation of the parameters ρ, D_A and D_k, while the absolute value of the angle ω is now obtained as:

$$\omega = \rho - \theta \tag{71}$$

with k given by:

$$k = D_k \sin(\omega) \tag{72}$$

The third possible situation is presented in Fig. 10 c), where the base station is higher than building A. With respect to the cases mentioned before, the angle ω is calculated as:

$$\omega = \theta + \rho \tag{73}$$

The values of k and D_k are obtained respectively from equations (68) and (69).

The separate diffraction losses are then summed in natural units, to the reflection loss (also in natural units), to get the overall clutter loss affecting one ray according to equation (58).

5.5 Reflection loss

The main part of the reflection calculation determines whether there is a reflected ray, and if it does exist, whether it is the result of one or more reflections.

Figure 11 illustrates in more detail the methodology to calculate the reflections undergone by the ray; the process starts by considering the nearest two buildings to the base station: if the ray passes over both buildings, there is no reflected ray and the process stops; otherwise, the methodology consists in capturing all possible reflections on the following buildings, which are generated by randomly extracting their distances and heights according to what is described in § 5.4. Each reflection on the buildings 3 to K is considered until the ray passes over the roof of the K+1-th building: the process ends as the ray is assumed to reach the satellite, with no further reflections. For each building, the horizontal distances are obtained as described in § 4.1. The losses due to all reflections are summed in dB. In addition, the impact of the ground is added (in case of negative elevation angles) by adding the loss associated to the reflection on the terrain.

FIGURE 11

Flow chart for determining the reflections

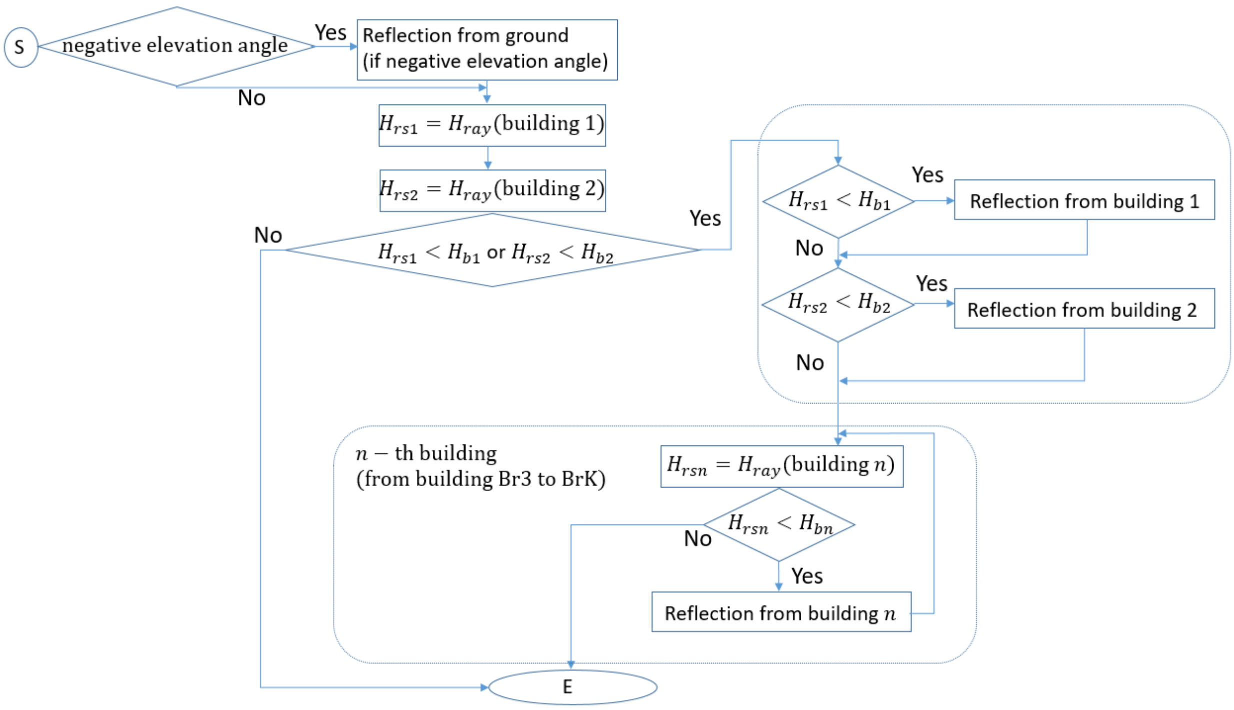

If there is no reflected ray, no reflection loss is calculated and the calculation should continue from § 5.7, except for negative elevation angles, for which the ground reflection loss has to be taken into account. Otherwise, the loss due to every reflection (both for ground and buildings) is calculated as a function of the reflection coefficient at the interface, considering two orthogonal linear polarizations. In fact, as is clear from the mathematical framework reported in Recommendation ITU-R P.2040, which describes the refraction and reflection of plane waves on planar discontinuities, the reflection coefficients are a function of the incidence angle, which, in turn, depends on both the horizontal and vertical angles defined in Fig. 12 (right side): the wave emitted by the base station might hit a building from quite different directions. This is clarified by the left side of Fig. 12, which depicts the incidence geometry for two sample rays having the same elevation angle ψ_S and different horizontal angles ϕ_S.

Making reference to the right side of Fig. 12, where the building façade is parallel to the *xz* plane, the incidence angle is calculated as:

$$\beta = \cos^{-1}[\cos(\psi_s)\cos(\phi_S)] \qquad \text{(degree)} \qquad (74)$$

FIGURE 12

Incidence of two sample rays having the same elevation angle and different azimuth angles

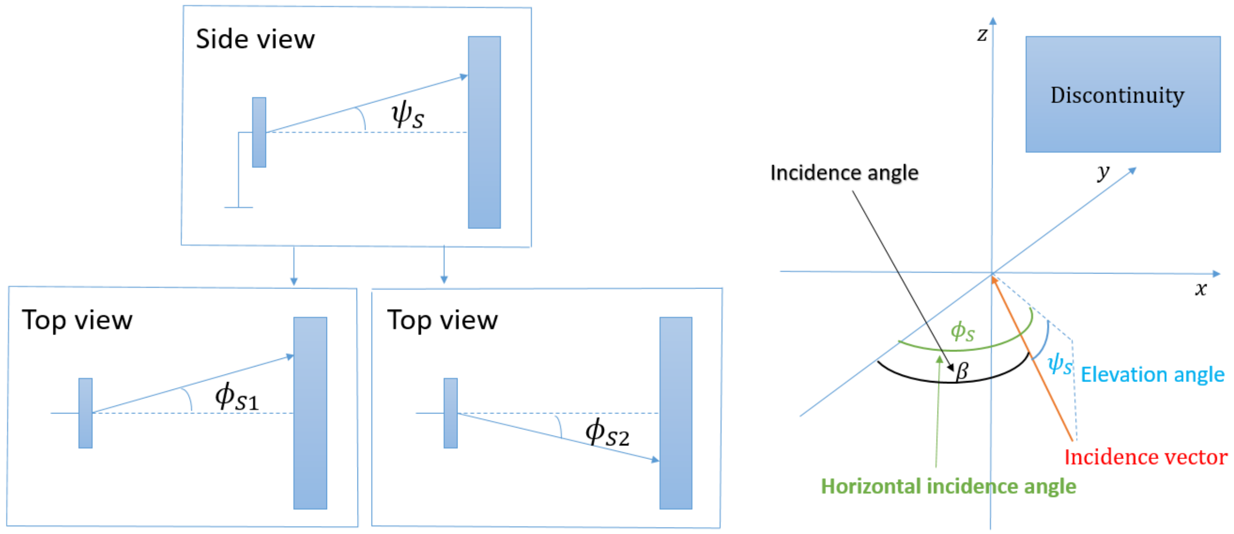

As clarified in Recommendation ITU-R P.2040, and as assumed in the method presented in this Report, two orthogonal polarizations, i.e. TE and TM, need to be taken into account: in fact, the reflection coefficient is calculated separately for both cases as a function of the wave frequency, the incidence angle, and the electromagnetic features of the material composing the building/ground, which might consist of multiple slabs of different media. The electromagnetic properties of each material are completely defined by the electric permittivity ε, the magnetic permeability μ and the conductivity σ: such values can be found in Recommendation ITU-R P.2040 (except for asphalt for which the value was derived from https://gprrental.com/gpr-velocity-table-analysis/) for different materials of typical buildings and ground, as a function of the frequency. In addition, as for some of the reflections due to the ground, the additional electro-magnetic parameters listed in Table 1 can be used.

TABLE 1

Electromagnetic parameters of asphalt, concrete, brick and glass (materials with relative magnetic permeability = 1) and their validity frequency range (*f*, expressed in GHz)

Material	***c***	***d***	**Conductivity σ (S/m)**	***a***	***b***	**Complex dielectric relative permittivity ε**	**Frequency range *f* (GHz)**
Asphalt	–	–	0.005	–	–	4.5 – *j*0.05	6-10
Concrete	0.032 6	0.809 5	$c\,f^d$	5.31	0	$a\,f^b - j\,17.98\,\sigma/f$	1-100
Brick	0.038	0	$c\,f^d$	3.75	0	$a\,f^b - j\,17.98\,\sigma/f$	1-10
Glass	0.004 3	1.192 5	$c\,f^d$	6.27	0	$a\,f^b - j\,17.98\,\sigma/f$	1-100

Recommendation ITU-R P.2040 also defines the complete procedure to calculate the reflection coefficients both for simple interfaces considering two materials (e.g. air-glass), as well as interfaces considering more complex materials consisting of multiple media (e.g. air-concrete/brick structure). The following materials can be considered for reflections on buildings:

– *concrete/brick structure*: the structure, depicted in Fig. 13, is a mix of concrete and brick layers; it is the typical structure adopted for peripheral walls of buildings.

FIGURE 13

Concrete/brick structure

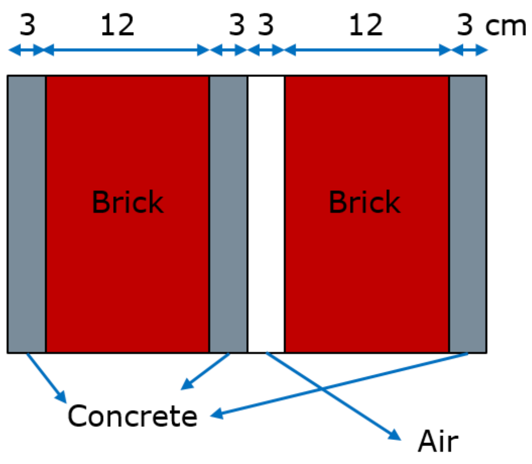

– *glass structure*: the structure, depicted in Fig. 14, consists of a single glass slab.

FIGURE 14

Glass structure

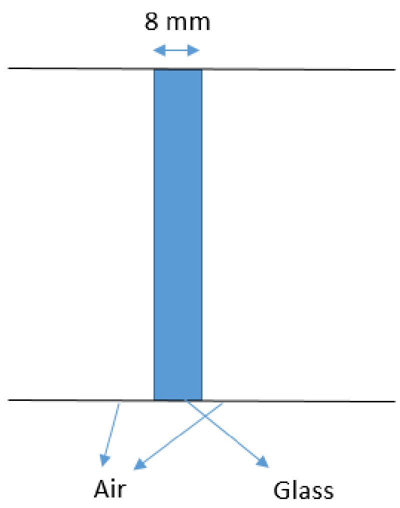

The following materials can be considered for reflections on dry ground:

– *dry asphalt*: simple interface with air.

– *dry paved*: simple interface with air.

– *dry vegetation*: simple interface with air.

– *dry grass*: the structure, depicted in Fig. 15, consists of the combination of dry grass and medium dry ground layers.

FIGURE 15

Dry grass structure

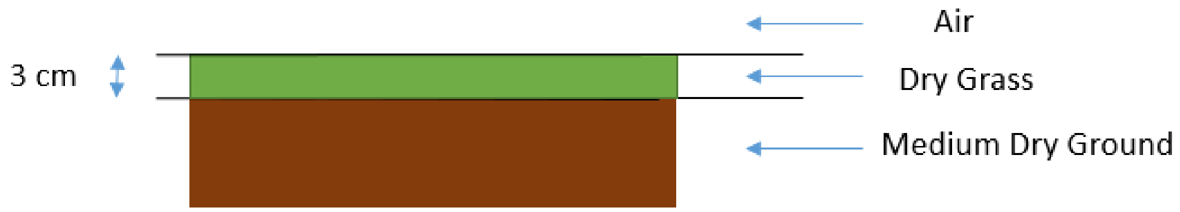

The following materials can be considered for reflections on wet ground:

– *wet asphalt*: simple interface with air.

– *wet paved*: simple interface with air.

– *wet vegetation*: simple interface with air.

– *wet grass*: the structure, depicted in Fig. 16, consists of the combination of wet grass and wet ground layers.

FIGURE 16

Wet grass structure

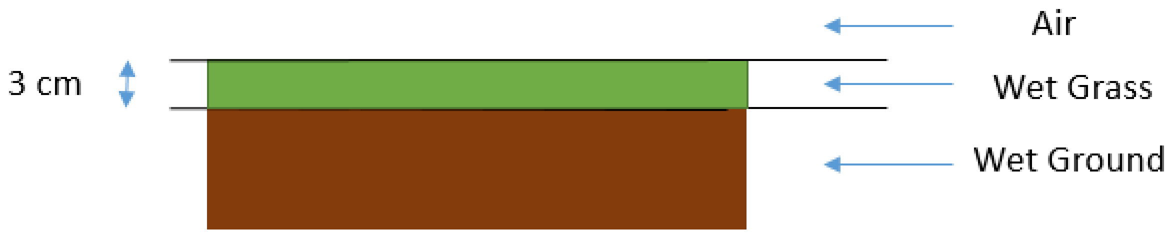

As example, Fig. 17 depicts the trend of the absolute value of the reflection coefficients, for both TM and TE components, as a function of the incidence angle. Results are shown for sample discontinuities: reflection from buildings (air-concrete/brick wall and air-glass slab) and from ground (air-dry asphalt). Overall, the TM component undergoes a lower reflection if compared to the TE polarization, especially around the Brewster's angle, for which the TM wave is totally refracted.

FIGURE 17

Trend of the absolute value of the reflection coefficient (both TE and TM cases) at 6 GHz as a function of the incidence angle, for different discontinuities: air to ground (asphalt) and building (concrete/brick wall and glass slab)

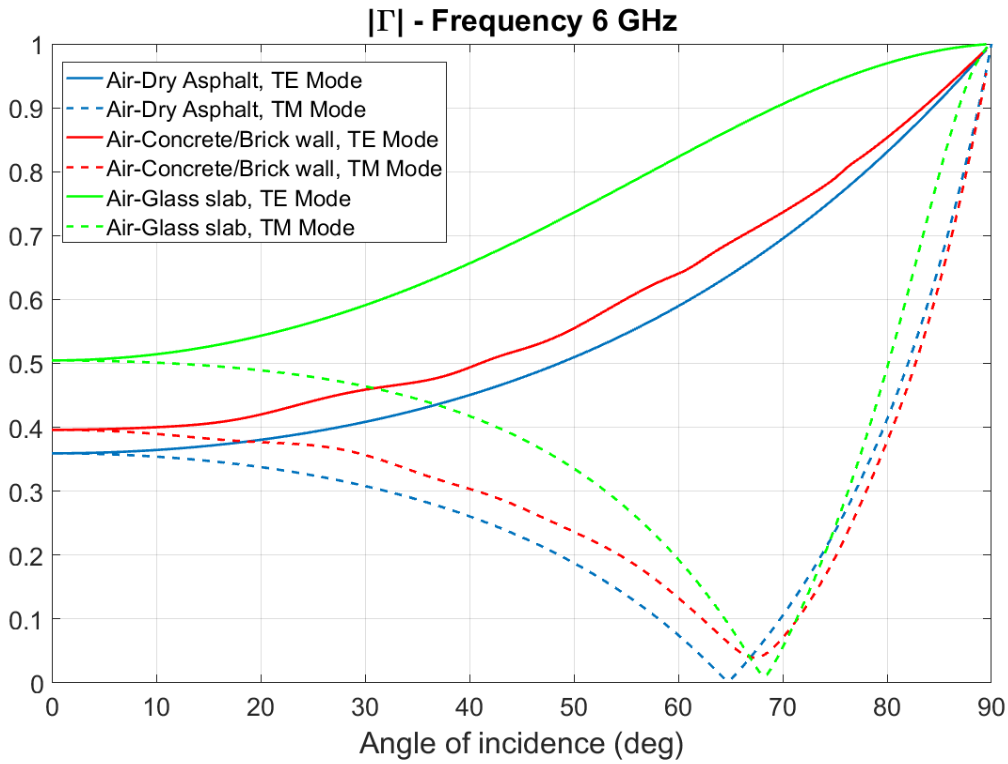

The squared reflection coefficient absolute value is transformed into the power loss as:

$$L_r = -10\log_{10}|\Gamma(f,\theta)|^2 \quad \text{(dB)} \tag{75}$$

Γ is the reflection coefficient depending on the frequency *f*, on the incidence angle θ, on the materials and on the polarization, calculated according to the mathematical framework described in Recommendation ITU-R P.2040.

5.6 Clutter loss

Each individual calculation accounts for one ray leaving the station, resulting in a single direct ray which may have diffraction loss, and possibly one reflected ray which may be the result of one or more reflections.

The clutter loss for each individual calculation depends on the following scenario:

– LoS case: in absence of building reflections, the overall clutter loss is calculated by multiplying the diffraction losses (in natural units) due to buildings B_1, B_2, B_{d3}, …, B_{dM}. In the case of a negative elevation angle, the overall clutter loss is also multiplied by the ground reflection loss. The overall clutter loss is then converted in dB using equation (57).

– NLoS case: the overall clutter loss is calculated by a combination of the losses associated with the two rays for each simulation according to equation (56). In the case of negative elevation angles, the overall clutter loss is also multiplied by the ground reflection loss. The overall clutter loss is then converted in dB using equation (57).

For each individual calculation the following parameters are calculated in natural unit for TE and TM polarizations and their average value between the two polarizations:

a) l_{cld}, total clutter loss of the direct ray, including reflection loss from front building, natural units.

b) l_{clg}, total clutter loss of the ray launched at elevation angle $-\theta$ and reflected from ground, natural units.

c) $l_{cl} = 1/\left(\frac{1}{l_{cld}} + \frac{1}{l_{clg}}\right)$, total clutter loss (see equation (18)), natural units[13].

5.7 Statistical output of the ray-launching stochastic method for clutter-loss

The stochastic model includes a statistical procedure that provides the following statistical outputs:

I) The cumulative distribution function of l_{cl}.

II) The cumulative distribution function of l_{cld}.

III) The cumulative distribution function of l_{clg}.

IV) The joint cumulative distribution function of l_{cld} and l_{clg}.

These outputs are provided as digital products which are integral to this Report. See description in Annex 1.

6 Application of the stochastic clutter-loss model

Results from repeated use of the stochastic calculation described in § 5 should be compiled into a cumulative distribution of clutter loss. Each calculation must use new random numbers for the probabilities; no random number should be used more than once.

For use with other propagation models and in spectrum-related studies it is convenient to compile the cumulative distribution in terms of percentage locations rather than probability.

The number of repetitions of the calculation for statistically reliable results can conveniently be judged by plotting the distribution at a scale which allows the required scale of accuracy to be visible. A smooth curve at this scale indicates that sufficient repetitions has been used.

The simulations are carried out both for two reference distributions, conventionally named as London and Melbourne at various frequencies, elevation angles and heights of the base station with 2×10^5 rays launched from the base station which is set, in the first simulation, with a randomly distributed height from the ground between 4 and 6 metres or, in the second simulation, with a height of 18 m. Half of the rays are associated with the TE polarization, the remaining part is launched with the TM polarization. The horizontal direction of the ray has been considered to be randomly distributed from 0 to 60 degrees, with respect to the normal of the buildings. Asphalt is the material used for the ground, while the buildings are modelled either using a concrete/brick structure or a glass slab: the stochastic process picks the glass incidence for 10% of the times, while the 90% of the building reflections are supposed to involve the concrete/brick walls.

---

[13] The parameter l_{cl}, total clutter loss is provided mainly for comparison with previous version of this Report and to provide a model reference value for comparison with measurements of basic transmission loss as defined in Recommendation ITU-R P.341.

7 Building statistics used to derive the reference clutter loss distribution

The distributions discussed in this chapter are available on Study Group 3 web page as an integral digital product.

7.1 Representative areas similar to The City, London, UK

The template used to produce the curves for areas similar to The City, London, UK was obtained from the survey points shown in Fig. 18. The city, London, is typical of a business centre with narrow streets and relatively few gaps between buildings. The survey points are on kerbs at the edge of pavements (sidewalks). To be typical of stations intended to serve small coverage areas, the locations mainly avoid street intersections.

FIGURE 18

Survey points in London

Table 2 gives the coordinates of the survey points.

TABLE 2

Coordinates of survey points in London

Point number	Latitude	Longitude
1	51°30'51.49"N	0° 5'14.98"W
2	51°30'48.34"N	0° 5'7.04"W
3	51°30'44.59"N	0° 5'5.59"W
4	51°30'44.66"N	0° 5'16.67"W
5	51°30'38.75"N	0° 5'4.31"W
6	51°30'38.94"N	0° 5'21.34"W
7	51°30'43.89"N	0° 5'9.57"W
8	51°30'46.19"N	0° 5'11.06"W
9	51°30'48.43"N	0° 4'55.80"W
10	51°30'44.21"N	0° 4'57.93"W
11	51°30'42.98"N	0° 4'50.27"W
12	51°30'39.32"N	0° 4'53.15"W

Figure 19 shows the distance and height cumulative distributions compiled from the survey points, constituting the template for central London.

FIGURE 19

Distance (right) and height (left) cumulative distributions for London
(The red line is the distribution of distance from survey point 1 to building 1;
the blue line is the distribution of distance from building 1 to building 2)

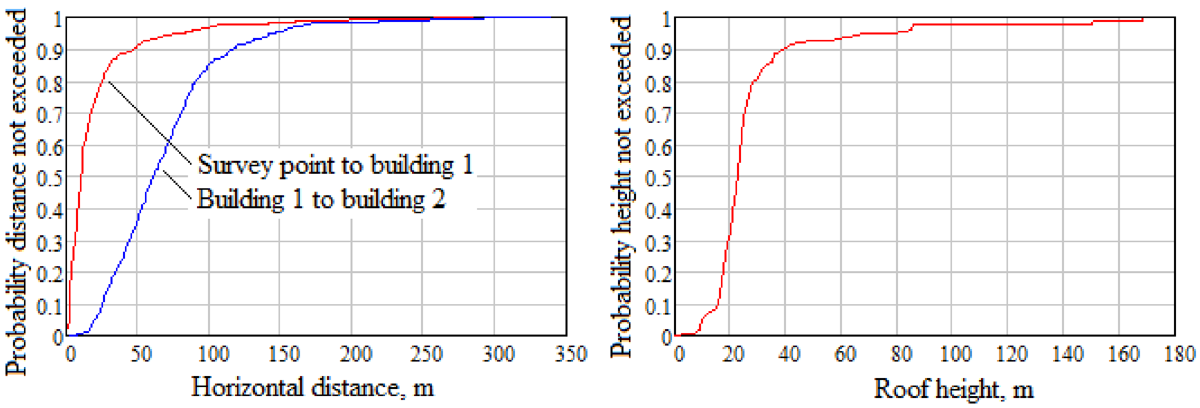

7.2 Representative areas similar to the central area of Melbourne, Australia

The template used to produce the curves for areas similar to the central area of Melbourne, Australia, was obtained from the survey points shown in Fig. 20. Central Melbourne is laid out on a rectangular grid with fairly wide main roads, but many narrow passages within the city blocks. To be typical of stations intended to serve small coverage areas, the survey point locations mainly avoid street intersections.

FIGURE 20

Survey points in Melbourne

Table 3 gives the coordinates of the survey points.

TABLE 3

Coordinates of survey points in Melbourne

Point number	Latitude	Longitude
1	37°48'48.23"S	144°57'28.00"E
2	37°48'50.46"S	144°57'30.09"E
3	37°48'53.17"S	144°57'30.93"E
4	37°48'56.13"S	144°57'33.33"E
5	37°48'58.88"S	144°57'35.31"E
6	37°49'3.95"S	144°57'35.88"E
7	37°48'57.06"S	144°57'43.55"E
8	37°48'52.31"S	144°57'42.84"E
9	37°48'49.81"S	144°57'37.43"E
10	37°48'46.72"S	144°57'39.34"E

TABLE 3 (*end*)

Point number	Latitude	Longitude
11	37°48'46.48"S	144°57'44.78"E
12	37°48'40.73"S	144°57'44.56"E

Figure 21 shows the distance and height cumulative distributions compiled from the survey points, constituting the template for central Melbourne.

FIGURE 21

Distance (left) and height (right) cumulative distributions for Melbourne (The red line is the distribution of distance from survey point 1 to building 1; the blue line is the distribution of distance from building 1 to building 2)

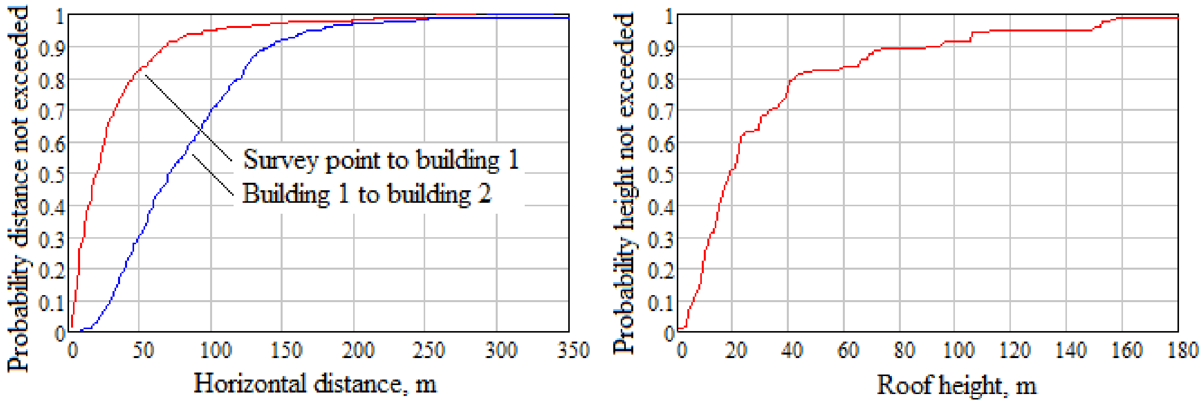

Annex 1

Description of the digital products integral to this report

These digital products are mentioned in Chapter 2, §§ 5.7 and 7 of this Report:

Statistical outputs

a) Digital products were generated using POLIMI stochastic model
POLIMI RL-Clutter issue 1 release 1 date 20/3/2025.
(Ray launcher implementing Chapter 2 of this Report).

b) Configuration parameters H_s, Transmitter
Height: 4..6, 8..10, 10..12, 12..14, 14..16, 16..18, 18..20, 20..22 and 22..24 m
f : 1, 3, 4 , 8, 10, 15, 23 GHz
City: London, Melbourne (see ref. distributions of H_b, D_{b1}, D_{b12})
θ = elevation angle, 5 to 85 degrees step 5 degrees)

c) Simulated parameters
Polarizations, TE, TM and (TE+TM)/2
Lcl (Effective Isotropic Clutter loss) dB
Lcl_d, (clutter loss direct ray, +θ) dB
Lcl_g (clutter loss ground reflected ray, −θ) dB

d) Output statistics
Cumulative distribution function of *Lcl*, total clutter loss, dB
Cumulative distribution function of Lcl_d, clutter loss of the direct ray, dB
Cumulative distribution function of Lcl_g, clutter loss of the ray reflected ray, dB
Joint Cumulative distribution function of Lcl_d and Lcl_g
Resolution: 0.5 dB, Range: 0..40 dB (*Lcl: −5..40 dB)*

e) File format

- CSV

f) Archive folder structure

<City>/<Freq GHz>/<Height-m>/<Polarization>/

Example: *./London/10/4-6/TE/*

g) File name: CDF_<parameter>_<Elev>.<suffix>

<Parameter> = **Lcl** or **Lcld** or **Lclg** or **Lcld** and **Llclg**

<Suffix> = **csv**

Example: *CDF_Lclg_05.csv*

h) Digital product Version history

- Issue 1, Rel. 0, date: 7/4/2025
  MAT files for CG 3K-3M-12 studies reference.
- Issue 1, Rel. 1, date: 29/4/2025
  MAT files for CG 3K-3M-12 studies reference.
- Issue 2, rel. 2,
  CSV File for ITU-R Rep. P.2402

i) Variables of Cumulative distributions

Column 1 = Parameter *x* (*Lcl* or *Lcld* or *Lclg)* [dB]

Column 2 = Probability *p* hat parameter in column 1 is not exceeded %, *CDF*(*x*)

j) Variables of Joint Cumulative distributions

The joint cumulative distribution is a 90 × 90 N_{ij} matrix, where
N_{ij}= number of samples when $y_i \leq L_{clg} < y_{i+1}$ and $x_j \leq L_{cld} < x_{j+1}$
and $N_t = \sum_{i=1}^{90} \sum_{j=1}^{90} N_{ij}$= total number of samples

- Line 1
  Column 1 = not used (set to Not a Number)
  Columns from 2 to 92 = values x_j of L_{cld} [dB], where *j* ranges from 1 to 91
- Lines from 2 to 91
  column 1 = value y_i of L_{clg} [dB], where *i* ranges from 1 to 90
  columns *j* from 2 to 91 = N_{ij}
- Lines 92
  column 1 = value y_{91} of *Lclg* [dB],

Note:

$Prob(L_{cld} < x_{j+1}) = \frac{1}{N_t} \sum_{k=1}^{90} \sum_{l=1}^{j} N_{kl}$, where *j* ranges from 1 to 90

$Prob(L_{cld} < x_{j+1}, L_{clg} < y_{i+1}) = \frac{1}{N_t} \sum_{k=1}^{i} \sum_{l=1}^{j} N_{kl}$,where *i* and *j* range from 1 to 90

$Prob(L_{clg} < y_{i+1} | L_{cld} < x_{j+1}) = \frac{Prob(L_{cld}<x_{j+1}, L_{clg}<y_{i+1})}{CDF(L_{cld} \leq x_{j+1})}$ where *i* and *j* range from 1 to 90

Building statistics

a) File formats

i. CSV

b) Folder Name: RepP2402_City-Stats

c) File name: <City>Stats.<suffix>

i. <City> = **London** or **Melbourne**

ii. <Suffix> = **csv**

iii. Example: *LondonStats.csv*

d) Variables

Column 1 = Hb, Roof height, m

Column 2 = PHb, Probability that Hb is not exceeded, %

Column 3 = Db1, distance from survey point to building 1, m

Column 4 = PDb1, Probability that Db1 is not exceeded, %

Column 5 = Db12, distance from building 1 to building 2, m

Column 6 = PDb12, Probability that Db12 is not exceeded, %

e) Digital product Version history

- Issue 1, Rel. 0, date: 7/4/2025
  MAT files for CG 3K-3M-12 studies reference.
- Issue 1, Rel. 1, date: 29/4/2025
  MAT files for CG 3K-3M-12 studies reference.
- Issue 2, rel. 2,
  CSV File for Report ITU-R P.2402

Annex 2

Application of the ray launching stochastic method of Chapter 2 to interference analyses

This Annex provides general information for the application for interference analyses of the method and digital products described in Chapter 2 and Annex 1.

A) Random draw of clutter loss components

The random draw of the components of the clutter loss, L^*_{cld} in dB (direct ray) and L^*_{clg} in dB (ground reflected ray) can be obtained with this procedure.

Input data:

- Digital table with joint distribution of Lcl_d and Lcl_g, $Q_j(\overrightarrow{P_{lcl}}, \overrightarrow{Lcld}, \overrightarrow{Lclg})$, formed by vectors $\overrightarrow{Lcld}$, $\overrightarrow{Lclg}$ and $\overrightarrow{P_{lcl}}$ with values of Lcl_d, Lcl_g and their associated probabilities of joint exceedance.

- Digital table with marginal distribution of Lcl_d, $Q_d(\overrightarrow{P_{lcld}}, \overrightarrow{Lcld})$, formed by vectors $\overrightarrow{Lcld}$ and $\overrightarrow{P_{lcld}}$ with values of Lcl_d and their associated probabilities of exceedance.

Steps:

a) Draw a random number P, Probability of exceeding values L^*_{cld} and L^*_{clg} with $0 \leq P < 1$.

b) Draw a random number P_{cld}, Probability of exceeding value L^*_{cld} with $0 \leq P_{cld} < 1$.

c) Derive value L^*_{cld} in dB using the table of the marginal distribution of L_{cld}: $L^*_{cld} = Q_d(\overrightarrow{P_{lcld}} = P_{lcld}, \overrightarrow{Lcld})$.

d) Derive value L^*_{clg} in dB using the table of the joint distribution of L_{cld} and L_{clg}: $L^*_{clg} = Q_j(\overrightarrow{P_{lcl}} = P, \overrightarrow{L_{cld}} = L^*_{cld}, \overrightarrow{Lclg}))$.

e) Convert L^*_{cld} and L^*_{clg} in dB to l^*_{cld} and l^*_{clg}, in natural units:

$$l^*_{cld} = 10^{\frac{L^*_{cld}}{10}}$$

$$l^*_{clg} = 10^{\frac{L^*_{clg}}{10}}$$

B) Power received by the antenna of the station in space

It is assumed that the transmitting station on the Earth uses an antenna A with a gain pattern $g(\theta, \phi)$ and an antenna boresight direction (θ_b, ϕ_b) with $g(\theta_b, \phi_b) = Max(g(\theta, \phi))$[14]. The gain of the antenna along the directions of the two launched rays are $g_1 = g(\theta - \theta_b, \phi - \phi_b)$ and $g_2 = g(-\theta - \theta_b, \phi - \phi_b)$. All antenna gains are in natural units.

The power received at the output of the receiving antenna in space is:

$$p_R(\theta, \phi) = p_t \cdot \left(\frac{g_1}{l^*_{cld}} + \frac{g_2}{l^*_{clg}}\right) \cdot g_r(\theta, \phi) \cdot \left(\frac{\lambda}{4\pi \cdot d}\right)^2 \quad \text{W}$$

where p_{t1} and p_{t2} in watt are values of input power to the antennas transmitting along directions θ and −θ, respectively, λ is the wavelength m, d is the distance from the station on the Earth to the station in space, $g_r(\theta, \phi)$ is the gain antenna of the station in space, l^*_{cld} and l^*_{clg} are the realisations of the clutter losses of the direct and ground reflected rays.

Annex 3

Application of the procedure of Annex 2 to a combination of different clutter scenarios

This Annex provides a procedure to derive the distribution of clutter losses for the application of Annex 2 to the case of a combination of *N* separate reference clutter scenarios (e.g. describing different parts of a large city or different cities).

[14] This expression uses the reference system of the station on ground.

Input data:

For each scenario *i*, with *i* ranging from 1 to *N*:

Q_{ji}: Digital Table with joint distribution of Lcl_d and Lcl_{gf} of scenario A.

Q_{di}: Digital Table with marginal distribution of Lcl_d of scenario A.

P_i: Probability of occurrence of scenario A.

Steps:

a) Derive Q_j the digital table with joint distribution of Lcl_d and Lcl_{gf} of the combined scenario

$$Q_j = \sum_{i=1}^{N} P_i \cdot Q_{ji}$$

b) Derive Q_d the digital table with marginal distribution of Lcl_d of the combined scenario

$$Q_d = \sum_{i=1}^{N} P_i \cdot Q_{di}$$

c) Use the procedure of Annex 2, using Q_j and Q_d to derive realisations of l^*_{cld}, l^*_{clg} and $p_R(\theta, \phi)$ in the combined scenario.

Annex 4

Summary of the characteristics of ray launching stochastic models

TABLE A4-1

General characteristics of stochastic model using ray-launching

Parameter	Description	Rep. ITU-R P.2402-0	Rep. ITU-R P.2402-1 Chapter 2	Uvigo model
N_L	Number of rays launched from the TX	1	2	4
n_i	Number or rays traced for each launched ray	2	2	2 for ray 1, 1 for rays 2, 3 and 4
n_G	Number of rays undergoing first reflection from ground	0	1	2
n_B	Number of rays undergoing first reflection from building	1	1	2
$n = n_B + n_G$	Number of rays originated by reflection	1	2	4
Azimuth dependence		No	Yes	No
n_d	Max number of diffractions along direct path	2	2	Up to 5
n_r	Max number of reflections	2	Variable+	2

TABLE A4-1 (*end*)

Parameter	**Description**	**Rep. ITU-R P.2402-0**	**Rep. ITU-R P.2402-1 Chapter 2**	**Uvigo model**
n_{rdr}	Max number of diffractions after reflection	0	2	Up to 5
Type of urban environment		Random (height and distances)	Random (height and distances)	Regular grid with random orientation and heights
Reflection loss model		ad-hoc, depends only on frequency, 8 dB or more No polarization	Ref. Rec. ITU-R P.2040 TE, TM and (TE+TM)/2	Same as Rep. ITU-R P.2402-0 plus randomisation factor
Diffraction model		KED	KED	KED
Diffraction from multiple buildings		KED + correction for double isolated edges	KED for isolated edges	Bullington
Conservation of total power along paths from a single ray		No	Yes	Yes
Combination of clutter loss of all rays		Yes	Yes	Yes
Negative clutter loss		Yes	Yes	Yes
Verification of the model with ray tracing		No	Yes[15]	On-going

\+ Recalculated for each realization of the Monte-Carlo simulation until the ray is above the last drawn building.

TABLE A4-2

Comparison of propagation effects of received rays in Reports ITU-R P.2402-0, P.2402-1 and UVigo model

Received ray	**Rep. ITU-R P.2402-0**	**Rep. ITU-R P.2402-1, Chapter 2**	**UVigo**
ray_d	• Diffraction from front building • Diffraction from other buildings (up to 2)	• Diffraction from front and next building	• Diffraction from front building • Diffraction from other buildings (up to 5)

15 See Systems. Electronics 2023, 12, 186. https://doi.org/10.3390/electronics12010186

TABLE A4-2 (*end*)

Received ray	Rep. ITU-R P.2402-0	Rep. ITU-R P.2042-1, Chapter 2	UVigo
ray_{Rd}	• Reflection from front building or buildings behind it along direct path • Reflection from rear building • No other reflections • Diffraction from other buildings (up to 2)	• Reflection from front building • Reflection from rear building • Other reflections	• Reflection from front building • Reflection from rear building • No other reflections • Diffraction from other buildings (up to 5)
ray_{R2}	• No ground reflection	• Reflection from ground • Diffraction from front and next building • Reflection from rear building • Other reflections	• Reflection from ground • Diffraction along direct path • No reflection from rear building • No other reflections • Diffraction from other buildings (up to 5)
ray_{R3}	• No fixed rear building (1)	• No fixed rear building (1)	• Reflection from rear building • Diffraction from front building • Diffraction from other buildings (up to 5)
ray_{R4}	• No fixed rear building (1)	• No fixed rear building (1)	• Reflection from ground • Reflection from rear building • Diffraction from front building • Diffraction from other buildings (up to 5)

(1) It is represented in the distribution of clutter losses by separate realisations of ray_{R11} and ray_{R12} (Chapter 2, Fig. 7, schema of survey points for urban statistics).

Annex 5

Summary of the reference scenarios of the Report

The models presented in this Report are based on different scenarios of clutter environment. This Annex presents a summary of the parameters of these scenarios and their use by the models.[16]

---

[16] Legend: Fit = Model fitting, MC = Monte-Carlo Simulations, NP = not provided, RL = Ray Launching, RT = Ray Tracing, VAL = Model Validation.

A) Scenarios for LOS probability in Recommendation ITU-R P.2108 (see Chapter 1, § 3.3.2)

Parameter	**Percentile**	**Sydney Australia**	**London UK**	**Shibuya Japan**	**Paris France**
H_b	50	7	18	23	NP
	95	18	28	63	NP
Map size (km × km)		4 × 4	2 × 2	1.5 × 1.5	2 × 2
Use		RT + Fit	RT + Fit	RT + Fit	VAL
P.2108 classification		Low-rise	Mid-rise	High-rise	NP

B) Scenarios for distribution of clutter loss in Recommendation ITU-R P.2108 (see Chapter 1, § 5.1.1)

Parameter	**Percentile**	**Phoenix USA**	**London UK**	**Beijing China**
H_b	50	4.35	14	24
Map size (km × km)		0.87 × 0.87	0.87 × 0.87	1.1 × 1.1
Use		RT + Fit	RT + Fit	RT + Fit
P.2108 classification		Low-rise	Mid-rise	High-rise

C) Scenarios for stochastic model in Report ITU-R P.2402 (Chapter 2)

Parameter	**Percentile**	**Melbourne Australia**	**London UK**
H_b	50	19	23
	95	149	76
D_{b1}	50	20	11
	95	110	74
D_{b12}	50	71	61
	95	180	147
Survey area (km × km)		0.81 × 0.81	0.74 × 0.74
Use		MC + RL	MC + RL
P.2108 classification		Mid-rise	High-rise